Transcription Factors DksA and PsrA are synergistic contributors to *L. pneumophila* virulence in *Acanthamoeba castellanii* protozoa

CHRISTOPHER I. GRAHAM, ANDREW J. GIERYS, TEASSA L. MACMARTIN, TIFFANY V. PENNER, JORDAN C. BECK, GERD PREHNA, TERESA R. DE KIEVIT and ANN KAREN C. BRASSINGA†

Department of Microbiology, Faculty of Science, University of Manitoba, Winnipeg, Manitoba, Canada R3T 2N2

Running Title: Regulatory synergy of DksA and PsrA in *L. pneumophila*

Keywords: *L. pneumophila*, stringent response, regulatory network, transcription factor, host-microbe interaction, biphasic lifestyle

†Corresponding author: Dr. Ann Karen C. Brassinga
Department of Microbiology (Fort Garry Campus)
Room 213, Buller Building
45 Chancellor's Circle
University of Manitoba
Winnipeg, MB, Canada
R3T 2N2
Phone: (204) 799-8457
E-mail: Ann.Brassinga@umanitoba.ca

Abstract

The environmental bacterium *Legionella pneumophila*, an intracellular parasite of free-living freshwater protozoa as well as an opportunistic human pathogen, has a biphasic lifestyle. The switch from the vegetative replicative form to the environmentally resilient transmissive phase form is governed by a complex stringent response-based regulatory network that includes RNA polymerase co-factor DksA. Here we report that, through a dysfunctional DksA mutation (DksA1), a synergistic interplay was discovered between DksA and transcription regulator PsrA using the *Acanthamoeba castellanii* protozoan infection model. Surprisingly, *in trans* expression of PsrA partially rescued the growth defect of a *dksA1* strain. While *in trans* expression of DksA expectantly could fully rescued the growth defect of the *dksA1* strain, it could also surprisingly rescue the growth defect of a Δ*psrA* strain. Conversely, the severe intracellular growth defect of a Δ*dksA* strain could be rescued by *in trans* expression of DksA and DksA1, but not PsrA. *In vitro* phenotypic assays show that either DksA or DksA1 were required for extended culturability of bacterial cells, but normal cell morphology and pigmentation required DksA only. Comparative structural modeling predicts that the DksA1 mutation affects coordination of Mg^{2+} into the active site of RNAP compromising transcription efficiency. Taken together, we propose that PsrA transcriptionally assists DksA in the expression of select transmissive phase traits. Additionally, *in vitro* evidence suggests that the long chain fatty chain metabolic response is mediated by PsrA together with DksA inferring a novel regulatory link to the stringent response pathway.

54 **Introduction**

55 *Legionella pneumophila*, a Gram-negative gammaproteobacterium, is commonly found in piped
56 water distribution systems where it is found as an intracellular parasite of free-living
57 bacterivorous protozoa (Rowbowtham, 1986; Steinert *et al.,* 2002; Newton *et al.,* 2010). These
58 environments are not only amenable to bacterial colonization and proliferation, but can also
59 aerosolize *Legionella*-laden water droplets that can be inhaled by susceptible individuals, thereby
60 facilitating bacterial infection of alveolar macrophages resulting in the atypical pneumonia
61 Legionnaires' disease (Newton *et al.,* 2010; Oliva *et al.,* 2018; Mondino *et al.,* 2020).

62 *L. pneumophila* is well adapted for its intracellular lifestyle in protozoa, and these
63 adaptations also enable human infection due to highly conserved eukaryotic cellular biology
64 (Newton *et al.,* 2010; Mondino *et al.,* 2020). A core driver of infection is the Dot/Icm Type IV
65 secretion system (T4SS), an apparatus that enables secretion of a diverse repertoire of ≥ 330
66 effectors into the host cytoplasm that together act to modify host cellular physiology upon uptake
67 of the bacteria (Finsel and Hilbi, 2015; Burstein *et al*., 2016; Gomez-Valero *et al.,* 2019). Such
68 modifications include subversion of phagosome trafficking to prevent fusion of the bacteria-
69 containing phagosome with lysosomes, and conversion of the phagosome into a replicative niche
70 referred to as the *Legionella*-containing vacuole (LCV) (Tilney *et al.,* 2001; Kagan and Roy,
71 2002; Isberg *et al*., 2009). As infection progresses within a protozoan host cell, *L. pneumophila*
72 exhibits a biphasic lifecycle, alternating between a vegetative replicative phase (RP) forms found
73 primarily in the LCV, and transmissive phase (TP) forms that develop upon depletion of host-
74 derived nutrients in anticipation of bacterial release to the environment. The physiology and
75 ultrastructure of TP cells is optimized for environmental survival and resistance to stress, with

76 expressed virulence factors enabling infection of a new host (Molofsky and Swanson, 2004;
77 Robertson *et al*., 2014; Oliva *et al.,* 2018).
78 The biphasic switch between RP and TP is controlled by a stringent response-based
79 regulatory network activated by accumulation of alarmone guanosine tetraphosphate (ppGpp),
80 which is synthesized by RelA and SpoT in response to nutritional deprivation. Synthase RelA
81 senses low amino acid concentrations (Zusman *et al.,* 2002), whereas bifunctional synthase and
82 hydrolase SpoT senses fatty acid flux via acyl carrier proteins (ACP) (Edwards *et al.,* 2009;
83 Dalebroux *et al.,* 2010). Accumulated ppGpp is associated with activation of the LetA/LetS two
84 component system (TCS), which in turn induces transcription of non-coding RNAs (ncRNAs)
85 RsmY and RsmZ (Hammer *et al.*, 2002; Rasis and Segal, 2009; Sahr *et al.,* 2009; Nevo *et al.,*
86 2014). These ncRNAs target and sequester the RNA-binding protein CsrA, thus modulating
87 CsrA-mediated post-transcriptional regulation of transcripts associated with the transition to TP.
88 Such transcripts include those encoding Dot/Icm effectors and those linked to cellular
89 metabolism (Häuslein *et al.,* 2017*;* Sahr *et al*., 2017). Other TCS also play a pivotal role in
90 bacterial differentiation and are often required for virulence in host cells, such as CpxR/A
91 (Feldheim *et al.,* 2016; Tanner *et al.,* 2016); PmrA/B (Zusman *et al.,* 2007; Al-Khodor *et al.,*
92 2009) and quorum sensing via LqsS/T/R (Tiaden *et al.,* 2007; Tiaden *et al.,* 2008; Schell *et al.,*
93 2014; Personnic *et al.,* 2018). In addition, a subset of transcriptional regulators plays an
94 important role in TP induction. IHF assists LetA in the upregulation of RsmY and RsmZ, and is
95 required for full cyst-like form differentiation and virulence in *A. castellanii* (Morash *et al*.,
96 2009; Pitre *et al*., 2013). OxyR regulates transcription of the operon encoding the CpxR/A TCS,
97 linking it to virulence in *A. castellanii* (Tanner *et al.,* 2017). Recently, the autorepressor PsrA
98 was found to be required for optimal intracellular growth and cyst-like form biogenesis in *A.*

99 *castellanii* (Graham *et al*., 2021). While the genetic targets of PsrA have not yet been identified,
100 a potential linkage between PsrA and the core stringent response network has been described
101 with focus on fatty acid flux and an associated ACP (Graham *et al.,* 2021).
102 Accumulated ppGpp also directly affects transcriptomic changes associated with the
103 transition from RP to TP. For example, expression of stationary phase sigma factor RpoS is
104 increased (Dalebroux *et al*., 2010), which is required for the expression of TP traits and
105 intracellular growth in protozoa such as *A. castellanii* (Hales and Shuman, 1999; Bachman and
106 Swanson, 2001; Zusman *et al.,* 2002; Abu Zant *et al.,* 2006; Hovel-Miner *et al.,* 2009). While the
107 precise mechanism has not yet been ascertained in *L. pneumophila*, ppGpp influences expression
108 most likely by binding directly to RNA polymerase (RNAP), as has been described in *E. coli*
109 where ppGpp binds with equal affinity either to a site encompassed by the ω and β' subunits, or
110 at the interface between RNAP and secondary channel co-factor DksA. DksA features a pair of
111 conserved aspartate residues to enable ppGpp binding (Perederina *et al.,* 2004; Ross *et al*., 2013;
112 Ross *et al*., 2016; Myers *et al*., 2020). The latter event results in a conformational change in both
113 ppGpp and DksA affecting the stability of the open complex generated by the RNAP
114 holoenzyme thereby altering the efficiency of transcription initiation (Chatterji *et al*., 1998;
115 Lemke *et al.*, 2011; Gummesson *et al.,* 2013; Ross *et al*., 2016; Molodtsov *et al.*, 2018; Travis
116 and Schumacher, 2021). DksA can act independently of ppGpp, compensate for its absence if
117 overexpressed, or even act antagonistically to ppGpp at different promoters (Magnussun *et al.,*
118 2007; Aberg *et al.,* 2008; Potrykus and Cashel, 2008; Aberg *et al*., 2009). DksA exists in a
119 dynamic equilibrium with structural homologs GreA and GreB in *E. coli*, which compete with
120 DksA for secondary channel binding. If either GreA or GreB binds, then DksA-independent
121 ppGpp binding to RNAP still occurs to influence expression (Vinella *et al.,* 2012).

122 *L. pneumophila* encodes both GreA and DksA orthologs, although GreA has not yet been
123 targeted for study. Like its *E. coli* ortholog, DksA acts independently of, or in coordination with,
124 ppGpp to regulate genes encoding TP traits (Dalebroux *et al.,* 2010). Previously, DksA was
125 shown to be required in a ppGpp-dependent manner for TP differentiation including flagellar
126 biosynthesis. Likewise, DksA and ppGpp are both required for optimal intracellular growth in *A.*
127 *castellanii*. Conversely, DksA, but not ppGpp, is dispensable for intracellular growth in murine
128 macrophages, indicating that ppGpp may act independently of DksA in *L. pneumophila*
129 (Dalebroux *et al.,* 2010). Thus, the contributions of ppGpp and DksA to the stringent response,
130 are well characterized among the proteobacteria though the mechanisms and targets may vary
131 between them (Gourse *et al*., 2018).
132 In this study, we describe an interplay between DksA and PsrA in the regulation of
133 virulence in protozoa, discovered through a hypomorphic mutant of DksA (DksA1). We show
134 that nominal intracellular growth can be fully achieved with DksA compensating for lack of
135 PsrA, but only partially achieved with PsrA supplementing DksA1, suggesting that PsrA
136 transcriptionally assists DksA. Structural modelling of DksA1 suggests that the transcription
137 efficiency of this RNAP co-factor is compromised, thereby highlighting the proposed synergistic
138 role of PsrA. Further, only DksA is essential for the *in vitro* phenotypic traits of extended
139 culturability, cell morphology and pigmentation. Conversely, *in vitro* evidence suggests that the
140 long chain fatty chain metabolic response is mediated by PsrA together with DksA. Taken
141 together, we show that PsrA and DksA have distinct and overlapping biological roles in the
142 regulation of TP highlighting a complex regulatory interaction between these two regulatory
143 factors.
144

145 **Methods**

146 **Structural Predictions and Modelling** The amino acid sequences of DksA and DskA1 were
147 submitted to the collabfold2 sever (Pettersen *et al*. 2021) with default settings. Top rank #1
148 models were selected for modelling and analysis in UCSF ChimeraX (Pettersen *et al*., 2021).
149 Structural overlays between Lp02 DksA, DksA1, and DksA (5VSW) (Molodtsov *et al*., 2018)
150 were aligned with Matchmaker. Conservation alignments were performed using Consurf
151 (Landau *et al*., 2005; Ashkenazy *et al*., 2016) with the Alphafold2 model of Lp02 DksA.

152

153 **Culture of *E. coli* and *L pneumophila*** *Legionella pneumophila* Philadelphia-1 derivative Lp02
154 parental and isogenic strains, as described in Table 1, were grown on Buffered Charcoal Yeast
155 Extract (BCYE) agar plates (Feeley *et al.*, 1979) at 37°C and 5% CO_2, or in Buffered-Yeast
156 Extract (BYE) broth in tubes on a roller drum at 37°C, supplemented as required with thymidine
157 (100 µg/mL), sucrose (5% w/v) or kanamycin sulphate (25 µg/mL). *E. coli* was utilized for
158 cloning and plasmid propagation purposes [DH5α for *in trans* expression vector pJB908 or pThy
159 (pBH6119), and DH5α λpir (suicide vector pSR47S) was grown on LB agar plates, or broth in
160 tubes on a roller drum, supplemented as required with ampicillin (100 µg/mL) or kanamycin
161 sulphate (40 µg/mL) and incubated at 37°C.

162

163 **Molecular methods/reagents, cloning, and sequencing** Chemicals were procured form VWR
164 (Ottawa, ON, Canada), Thermo-Fisher (Mississauga, ON, Canada), or Sigma-Aldrich (Oakville,
165 ON, Canada). Restriction endonuclease and PCR polymerase (Taq, Q5), and other cloning
166 reagents were procured from New England Biolabs (Whitby, ON, Canada). Oligonucleotide
167 primers, ordered from Life Technologies (Thermo-Fisher), were utilized under conditions listed

168 in Table 2. Nucleic acid purification kits were purchased from Qiagen (Toronto, ON, Canada).
169 Sanger sequencing for routine verification of constructs and mutant validations was done on a
170 fee-based service by The Centre for Applied Genomics (The Hospital for Sick Children,
171 Toronto, ON, Canada). Whole genome sequencing was undertaken by phenol-chloroform
172 isolation of genomic DNA followed by sequencing via Pacbio SMRT at Genome-Québec
173 (Montreal, QC, Canada) and assembled using Geneious™ software.
174
175 ***dskA1* and Δ*dksA* mutant strains** The *dksA1* mutation was identified through whole genome
176 sequencing of a Δ*psrA* mutant strain (i.e. *dksA1* Δ*psrA*) during experiments for Graham *et al.*
177 (2021). The *dskA1* mutation was then traced back to the electrocompetent cell stock to attain the
178 *dksA1* strain via PCR screening using primer set (PF dksA1 missing / PR dksA1 missing) that
179 annealed to the missing 24 bp region within *dksA1* in combination with primer set (PF dksA ext
180 conf / PR dksA ext conf). For these reactions, PF dksA1 missing was paired with PR dksA ext
181 conf, and PF dksA ext conf was paired with PR dksA1 missing, such that each primer set only
182 generated product to identify the *dksA1* allele. For generation of an in-frame Δ*dksA* mutant
183 strain, ~1000 bp 5′ (primer set PF 5-flk dksA SalI / PR 5-flk dksA BamH1) and 3′ (PF 3-flk
184 dksA BamH1 / PR 3-flk dksA SacI) regions flanking *dksA* were PCR-amplified and cloned into
185 suicide vector pSR47S to use for routine allelic exchange. For generation of *in trans* expression
186 constructs, either *dksA* or *dksA1* were PCR-amplified from Lp02 or *dksA1* mutant CG799,
187 respectively, using primer set (PF comp dksA BamHI / PR comp dksA SacI) and cloned into
188 pJB908, and introduced into parental or isogenic mutant strains by electroporation. The *in trans*
189 *psrA* expression vector was from a previous study (originally referred to as pComp henceforth
190 renamed to pVect-*psrA* in this study) (Graham *et al*., 2021). Use of pThy empty vector pBH6119

is used to rescue thymidine auxotrophy of Lp02. Plasmid constructs and mutations were routinely verified by sequencing isolated plasmids or PCR amplicon products, and mutant strains were routinely subjected to whole genome sequencing to rule out secondary mutations.

***In vitro* growth kinetics** *L. pneumophila* strains were grown on plates for three days under standard conditions. Bacterial cell mass was collected with a disposable loop and suspended in pre-warmed BYE broth and normalized to OD_{600} = 0.15. Subsequently 150 µL of this suspension was loaded in triplicate into wells within a 96-well flat bottomed microtitre plate, the lid was sealed with Parafilm, and loaded into a BioTek Synergy HTX plate reader, reading OD_{600} hourly for 24 h at 37°C or every 2 h for 48 h at 25°C with 150 rpm linear shaking. Results were plotted in GraphPad Prism™ 9.1 and analyzed via two-way ANOVA analysis.

Culture and intracellular kinetics in protozoan *A. castellanii* *Acanthamoeba castellanii* (ATCC 30234) were propagated in PYG media at 25°C as previously described (Tanner *et al.,* 2016). Briefly, infections were undertaken in AC buffer by placing ~10^6 protozoan trophozoites in each well of a set of tissue culture-treated 24-well plates and allowing them to adhere, then overlaying them with bacteria normalized by OD_{600} to a MOI of 0.1 in AC buffer. After 1 h incubation at 25°C, the wells were washed 3 x 1 mL AC buffer, before incubating in 1 mL/well of AC buffer at 25°C until the indicated timepoints. Protozoa were lysed mechanically via vortexing, and the lysate serially diluted in AC buffer onto BCYE-agar plates to enumerate titres. To enhance enumeration of difficult-to-recover avirulent strains, a portion of the lysate was tenfold concentrated by centrifugation at 21,000 x *g* in a microcentrifuge for 2 min, then 0.9 vol of the supernatant drawn off, the pellet resuspended in the remaining volume and spotted

214 alongside the serial dilutions. After counting titres, graphs were plotted and analyzed (two-way
215 ANOVA) in GraphPad Prism™ 9.1.
216
217 **Culture and intracellular kinetics in U937 human macrophages** Human U937 monocytic
218 cells were propagated and differentiated into macrophages using phorbol myristate acetate
219 (PMA, Sigma-Aldrich) as previously described (Tanner *et al.,* 2016). Cells were grown in
220 RPMI-1640 media (HyClone, Thermo-Fisher) supplemented with 10% heat inactivated fetal
221 bovine serum (Seradigm, Mississauga, ON) (RPMI + FBS) at 37°C and 5% CO_2 that was used
222 for all washes and incubations in a pre-warmed state. For infection, ~ 10^6 activated U937-derived
223 macrophages were placed into each well of a tissue culture-treated 24 well plate, allowed to
224 adhere, and overlaid with *L. pneumophila* strains normalized by OD_{600} to a MOI of 2, for 1 h.
225 The bacteria were washed away with 3 x 1 mL washes in RPMI + FBS, followed by an
226 incubation for 1 h with RPMI + FBS with 100 µg/mL gentamicin. After a further 3 x 1 mL
227 washes in RPMI + FBS, the cells were incubated in 1 mL RPMI + FBS until lysis at indicated
228 timepoints. Cells were lysed osmotically by replacing the RPMI + FBS with ice-cold HyClone
229 ultrapure water and repeated pipetting (Thermo-Fisher), then serially diluting the lysate in
230 additional HyClone water and enumerating *L. pneumophila* titres by spotting the dilutions on
231 BCYE-agar plates. After counting, graphs were plotted and analyzed via two-way ANOVA in
232 GraphPad Prism™ 9.1.
233
234 **Pigment, morphology and culturability assays** Suspensions of *L. pneumophila* were prepared
235 as per *in vitro* growth kinetics. Pigment assays were undertaken in accordance to Wiater et al.
236 (1994). Briefly, inoculated 5 mL BYE broth cultures were incubated for 72 h. To quantify

237 pigment at 24 h timepoints, 1 mL of culture was withdrawn, pelleted at 21,000 x g in a
238 microcentrifuge for 2 min, after which 150 µL of supernatant was loaded in triplicate into 96
239 well plates and read for absorbance at 550 nm on a BioTek Synergy HTX plate reader (Wiater *et*
240 *al*., 1994). After removal of residual supernatant, the pellet was suspended in 1 mL of 1 x PBS
241 pH 7.0 and similarly loaded (150 µL) into a 96 well plate then read for OD_{600}. Blank controls
242 were the same volume of BYE or 1 x PBS as appropriate. Results were plotted and analyzed
243 using GraphPad Prism™ (9.1). Photographed samples were prepared similarly and at specified
244 allowed to sit undisturbed for 24 h at ambient temperatures (~22°C) for cells to sediment out by
245 gravity. Long-term culturability was assessed by inoculating 96 well plates with six wells for
246 each strain, containing 150 µL of an OD_{600} = 0.15 suspension in BYE. The outermost rows and
247 columns were filled with sterile water to reduce evaporation, the plates were sealed with
248 Parafilm and incubated on a shaking platform at 37°C for four days. At indicated intervals, cell
249 aggregates were dispersed with pipetting, the OD_{600} was read with a BioTek Synergy HTX plate
250 reader across the wells containing unharvested culture, and one well of each strain harvested and
251 serially diluted for titre on BCYE agar plates. Results were plotted and analyzed using GraphPad
252 Prism (9.1). For colony-spot morphology, 10 µL of the residual OD_{600} = 0.15 suspension used to
253 prepare these assays was spotted on a BCYE plate with spots spread out to twice the spacing of a
254 standard multi-channel pipette then incubated for 4 days at 37ºC and 5% CO_2, then
255 photographed.
256
257 **LCFA assays** Suspensions of *L. pneumophila* strains were prepared as per the *in vitro* kinetics,
258 at OD_{600} = 0.15 in BYE broth, except that media was supplemented with two-fold serially diluted
259 concentrations of palmitic acid (PA) as a 40 mM stock dissolved in 100% ethanol. All broth

260 including PA dilutions, controls and blanks was normalized to 0.5% ethanol. The suspension was
261 then subject to a standard in vitro growth curve as described in the *in vitro* kinetics section.
262 Inhibition was defined as growth of <50% in comparison to that of the same strain in a BYE +
263 0.5% ethanol-only control at the end of 24 h. Data were graphed using GraphPad Prism™ 9.1.
264
265 **Microscopy** Microscopy and cell lengths were conducted as per Graham *et al.,* (2021). Briefly,
266 broth cultures in BYE broth were inoculated at OD_{600} = ~0.02 and incubated for 18 h to OD_{600} =
267 0.5-1.0 at 37°C to enter exponential phase, then were mounted on a 2% w/v agarose pad
268 prepared in water and imaged on an Axio Observer Z1 inverted microscope (Zeiss) equipped
269 with a glycerol-immersion 150X objective. Stationary phase cells were imaged by returning the
270 cultures to the roller drum for a further ~24 h to achieve stationary phase and imaged similarly.
271 Cell lengths were quantified using the length tool in ImageJ and lengths plotted and analyzed in
272 GraphPad Prism™ (9.1).
273
274
275
276
277
278
279
280
281
282

283 **Table 1** List of strains and plasmids

Number	Name	Description	Source/reference
E. coli			
	DH5α	F′ *endA1 hsdR17*(r_k- m_k-) *supE44 thi-1 recA1 gyrA* (*Nal*^{r}) *relA1* Δ(*lacZYA-argF*)*U169 deoR*(ϕ80lacΔ(lacZ)M15)	New England Biolabs
	DH5α λpir	K-12 F- φ80*lacZ*ΔM15 *endA recAhsdR17* (*rm-mK*+) *supE44 thi-1 gyrA96 relA1* Δ(*lacZYA-argF*) U169 *λpir*	M. Swanson (Bryan *et al*., 2013)
L. pneumophila			
C858	Lp02	Str^r, Thy$^-$, HsdR$^-$ derivative of Philadelphia-1 strain	M. Swanson (Berger and Isberg, 1993)
KB265	Lp03	Lp02 Δ*dotA* mutant	R. Isberg (Berger and Isberg, 1993)
CG859	Δ*psrA*	Lp02 Δ*psrA* (unmarked, in frame deletion mutant)	Graham *et al.,* (2021)
CG860	Lp02 pThy	Lp02 pBH6119	Tanner *et al*., (2016)
JT708	Δ*dotA* pThy	Lp03 pBH6119	Tanner *et al*., (2016)
CG861	Lp02 pVect-*psrA*	Lp02 pJB908-*psrA*	Graham *et al.,* (2021)
CG862	Δ*psrA pThy*	Δ*psrA* pThy	Graham *et al.,* (2021)
CG863	Δ*psrA* pVect-*psrA*	Δ*psrA* pJB908-*psrA*	Graham *et al.,* (2021)
CG799	*dksA1*	Lp02 *dksA1* (*dksA1*[Δ*170-194]*); spontaneous 24 bp in-frame deletion	This study
CG819	*dksA1* pThy	*dksA1* pBH6119	This study
CG813	*dksA1*Δ*psrA*	Lp02 *dksA1* Δ*psrA*	This study
CG826	*dksA1* Δ*psrA* pThy	*dksA1* Δ*psrA* pBH6119	This study
CG1053	Δ*dksA*	Lp02 Δ*dksA* (unmarked, in frame deletion mutant of *dksA*)	This study
CG1054	Δ*dksA* Δ*psrA*	Δ*dksA* Δ*psrA*	This study
CG1055	Δ*dksA* pThy	Δ*dksA* pBH6119	This study
CG1056	Δ*dksA* Δ*psrA* pThy	Δ*dksA* Δ*psrA* pBH6119	This study
CG1057	Δ*dksA* pVect-*dksA*	Δ*dksA* pBH6119	This study
CG1059	Lp02 pVect-*dksA*	Lp02 pJB908-*dksA*	This study
CG1060	Δ*psrA* pVect-*dksA*	Δ*psrA* pJB908-*dksA*	This study
CG1061	Δ*dksA* pVect-*psrA*	Δ*dksA* pJB908-*psrA*	This study
CG1101	Δ*dksA* pVect-*dksA1*	Δ*dksA* pJB908-*dksA1*	This study
CG1102	Lp02 pVect-*dksA1*	Lp02 pVect-*dksA1*	This study
CG1146	*dksA1* pVect-*dksA*	*dksA1* pVect-*dksA*	This study
Plasmids			
	pJB908	RSF1010 cloning vector, *td*Δ*i*, Amp^r Thy$^+$	J. Vogel (Sexton *et al*., 2004)
	pBH6119	RSF1010 promoterless GFP vector; Amp^r, Thy$^+$	M. Swanson (Hammer *et al*., 2002)
	pSR47S	oriTRP4 oriR6K *kan*^{r} *sacB*	J. Vogel (Merriam *et al*., 1997)
pPP619	pVect-*psrA*	pJB908-*psrA*	Graham *et al.,* (2021)

pCG1051	pVect-*dksA*	pJB908-*dksA*	This study
pCG1080	pVect-*dksA1*	pJB908-*dksA1* allele recovered from spontaneous *dksA1* Lp02 strain CG799	This study
pCG1069	pSR47S-5′flk-*ΔdksA*-3′flk	pSR47S with 5′ and 3′ flanking regions for Δ*dksA*	This study

284

285

286

287 **Table 2** List of oligonucleotides.

Name	Sequence	Annealing Temp. (ºC)	Product Size (bp)
Cloning/Confirmation			
PF 5-flk dksA SalI	gcgataGTCGACgttagaggcagaacttttactctg	62	915
PR 5-flk dksA BamH1	gcgataGGATCCatcaattaattgtcctgtcatgcc		
PF 3-flk dksA BamH1	gcgataGGATCCcagggtgcttgattctttcttg	62	978
PR 3-flk dksA SacI	gcgataGAGCTCgtaataagggctctgtagtgagg		
PF comp dksA BamHI	gcgataGGATCCgatttcagcaaagaggcattgg	62	1016 (*dksA*) 992 (*dksA1*)
PR comp dksA SacI	gcgataGAGCTCgaatcaagcaccctgattttgg		
PF dksA ext conf	caagcaatcggaataacaaacc	62	842
PR dksA ext conf	cactgtaagccttgttgattttc		
PR dksA conf int	gtcttgcttcaagacgtttcag	57.5	533 (with PF ext dksA conf)
pF dksA1 missing*	ggaagaagtagatcgtactgtctc	57.5	320 with pF ext dksA conf*
PR dksA1 missing*	gagacagtacgatctacttcttcc	57.5	546 to pR ext dksA conf*
Sequencing			
PF pSR47s seq	ctgttgcatgggcataaagttg	-	–
PR pSR47s seq	cacaggaaacagctatgacc	-	-
PF pJB908 seq	ctccgtgatggaatgacaac	-	–
PR pJB908 seq	gaccgcttctgcgttctga	-	–

288 Restriction sites indicated by capitalized letters.

289 * dksA1 missing primers used for screening strains, anneal to the region missing in *dksA1* and
290 will only generate product with the parental allele.

291

292

293

294

295

296

297 **Results**

298 ***dksA1* mutation** In a previous study, we deleted *psrA* from the parental Lp02 strain (Graham *et*
299 *al*., 2021). Throughout this process, we noted a propensity for some of the isogenic Δ*psrA* strains
300 to acquire secondary mutations in *letS* or *dksA* as discovered through routine whole genome
301 sequencing. One particular Δ*psrA* strain was found to contain an in-frame 24 bp deletion within
302 the *dksA* coding sequence, that resulted in the loss of eight amino acid residues after the 57th
303 residue in the DksA polypeptide (Figure S1A, B). The 57th codon was additionally altered from
304 encoding leucine to phenylalanine. Thus, this allele was denoted as the *dksA1* mutation that is
305 characterized in this study.

306 As the truncation appeared in the designated coiled-coil (CC) domain of DksA, we
307 investigated how the truncation could affect the fold of DksA1 using AlphaFold2 (Jumper *et al*.,
308 2021; Skolnick *et al*., 2021). The polypeptide sequences of DksA and DksA1 were submitted to
309 the colabfold2 server (AlphaFold2) with default settings and were modelled with a moderate-to-
310 high degree of confidence (Figure S1C, D). The CC domain of DksA was well built as was the
311 majority of the globular-head (GH) domain. Conversely, the eight-amino acid truncation in
312 DksA1 resulted in a partial disruption of the tip of the CC domain with AlphaFold predicting a
313 'disordered' loop with moderate confidence (Figure S1D). The extent of the potential structural
314 changes in the mis-formed tip of the CC domain in DksA1 can be observed when overlaid with a
315 previously solved structure of a DksA:RNAP complex from *E. coli* (PDB ID: 5VSW)
316 (Molodtsov *et al*., 2018). As shown in Figure 1A, all DksA variants align well, except for the
317 altered CC-loop regions near helix α3 and the C-terminal region helix α5 not present in the DksA
318 *E. coli* crystal structure. Importantly, the truncation did not delete key function residues shown to
319 be needed for interaction of DksA with the RNAP allosteric (K104, L101, K100, R97) or with

320 the RNAP active site (D80, D77) (Parshin *et al*., 2015; Molodtsov *et al*., 2018) (Figure 1B).
321 Furthermore, all DksA variant structures can be modeled into RNAP (Figure S2) slotting into the
322 allosteric site (Figure 1C) and RNAP active site (Figure 1D) without significant variation from
323 the experimental DksA structure. However, while the AlphaFold predictions for Lp02 DksA and
324 DksA1 had a properly modeled ppGpp binding site (Figure 1E), the twin-aspartate loop of the
325 CC domain was significantly altered in DksA1 through the shift of D69 (D71 in DksA) by ~8.9Å
326 (Figure 1F). These models therefore suggest that while the functional residues are conserved
327 from the truncation, DksA1 should be incapable of coordinating Mg^{2+} in the active site of
328 RNAP. Conversely, the structural predictions show that DksA1 is likely still able to bind RNAP.
329 Specifically, DksA1 is predicted to still contact the secondary binding site of ppGpp functionally
330 as an allosteric inhibitor of RNAP through ppGpp-mediated recruitment.
331

332 **PsrA partially rescues the growth defect of the *dksA1*, but not Δ*dksA*, strain in *A. castellanii***

333 Given the previously described regulatory roles of DksA and PsrA (Dalebroux *et al.,* 2010;
334 Graham *et al.,* 2021), the discovery of the Δ*psrA dksA1* strain along with the *dksA1* strain
335 presented a fortuitous opportunity to investigate potential regulatory links between the two
336 proteins in the established *A. castellanii* protozoan infection model. Intracellular growth kinetics
337 were conducted on *dksA1* pThy, Δ*psrA* pThy, *dksA1* Δ*psrA* pThy, and *dksA1* pVect-*psrA* strains,
338 along with virulent Lp02 pThy and avirulent Δ*dotA* pThy strains as controls, at 25ºC over 168 h
339 as previously described (Tanner *et al.,* 2016; Graham *et al*., 2021) (Figure 2A). The profiles of
340 Lp02 pThy and Δ*dotA* pThy strains were as expected demonstrating ~ three-$\log_{10}$ increases in
341 titre, and titres staying near initial inoculum concentration, respectively. The *dksA1* pThy and
342 Δ*psrA dksA1* pThy strains showed no significant increase in titres indicating that the

343 chromosomal single copy *dksA1* mutation was defective for virulence. Surprisingly, *in trans*
344 PsrA expression in the *dksA1* background resulted in a two-$\log_{10}$ recovery of growth ($p = 0.0006$)
345 to a titre within one-$\log_{10}$ of the Lp02 pThy strain. This suggested PsrA were able to partially,
346 but not fully, rescue the avirulent phenotype demonstrated by the *dksA1* strain. While a genomic
347 copy of *psrA* is present in the *dksA1* strain, it was shown previously that *in trans* expression of
348 PsrA from pVect-*psrA* resulted in an elevated quantity of cellular protein that not only rescued
349 the reduced growth phenotype associated with gene deletion of *psrA*, but also enhanced
350 replicative growth of Lp02 in *A. castellanii* (Graham *et al.*, 2021). Nevertheless, the surprising
351 ability of PsrA to partially complement the growth defect of *dksA1* led us to expand our
352 investigations to define the relationship between the two regulatory factors.

353 A previous study elsewhere reported that an insertional *dksA* mutant showed a modest
354 intracellular growth defect in *A. castellanii* at 37°C with slow growth initially, but eventually
355 achieving similar titres to Lp02 by the end of the 96 h experiment (Dalebroux *et al,* 2010). This
356 reported phenotype differs in comparison to the significantly reduced intracellular growth
357 observed with the *dksA1* strain in this study, thereby supporting our hypothesis that DksA1 bore
358 altered function and distinct phenotype versus the null mutant. To test this, and to determine if
359 the compensatory effect of *psrA* observed with the *dksA1* mutant strain extended to a null
360 deletion mutant strain, we generated single Δ*dksA* and double Δ*dksA* Δ*psrA* mutant strains. The
361 intracellular growth kinetics of the strains were assessed in *A. castellanii* under the same
362 conditions (Figure 2B). Interestingly, the Δ*dksA* pThy and Δ*dksA* Δ*psrA* pThy mutant strains
363 were both fully avirulent, starting at a slightly lower titre than the Δ*dotA* pThy strain, then
364 declining to, or below, the detection limit of the assay (~10 CFU/mL). The severe growth defect
365 of the Δ*dksA* pThy strain was fully rescued by *in trans* expression of *dksA*, but not *psrA*; a

366 notable divergence from the rescued phenotype demonstrated by the *dksA1* pVect-*psrA* strain.
367 Taken together, the lack of DksA results in a complete avirulent phenotype in these conditions
368 which cannot be rescued by PsrA, whereas the hypomorph DskA1 has a less severe impact on
369 intracellular growth that can be partially rescued by PsrA.
370
371 **DksA1 rescues the growth defect of the Δ*dksA* strain, and vice versa, in *A. castellanii*** Since
372 DksA can rescue the severe growth defect of the Δ*dksA* strain in *A. castellanii* (Figure. 2B), we
373 next asked if the partially functional DksA1 could likewise do so despite the truncation in the
374 coiled-coil structure (Figure 1). To answer this, the Δ*dksA* pVect-*dksA1* strain was assessed in *A.*
375 *castellanii* along with Δ*dksA* pThy, Lp02 pThy and Δ*dotA* pThy (Figure 2C). The severely
376 reduced growth phenotype of the Δ*dksA* pThy strain was robustly rescued by *in trans* expression
377 of DksA1 as shown by the growth profile of the Δ*dksA* pVect-*dksA1* strain ($p = 0.0002$)
378 matching that of the Lp02 pThy strain. It should be noted that this growth phenotype contrasted
379 with the minimal growth profile of the *dksA1* pThy strain (Figure 2A), suggesting that restoration
380 of the virulent phenotype of the Δ*dksA* strain was due to *in trans* expression of DksA1 protein
381 (pVect-*dksA1*) of sufficient levels to offset the structural and functional inefficiency. Not
382 unexpectantly, *in trans* expression of DksA successfully rescued the avirulent phenotype of the
383 *dksA1* pThy strain to match the growth profile of Lp02 pThy most likely due to the *in trans*
384 expression of DksA of which levels exceeded that of DksA1 (Figure 2D). In the reverse scenario,
385 the growth profile of Lp02 pVect-*dksA1* still matched that of Lp02 pThy suggesting that despite
386 the *in trans* expression of DksA1, the chromosomal-copy production levels of DksA and PsrA in
387 parallel were each sufficient to disguise any effects caused by the dysfunctional DksA1 (Figure
388 2A, Figure 2D).

DksA restores the growth defect of the Δ*psrA* strain in *A. castellanii* To further define the relationship between DksA and PsrA, we next asked if DksA could reciprocally compensate for lack of PsrA or generally, affect intracellular growth in the presence of PsrA. To answer this, Lp02 pVect-*dksA* and Δ*psrA* pVect-*dksA* strains were assessed for growth in *A. castellanii* along with the Lp02 pThy, Δ*dotA* pThy and the Δ*psrA* pThy strains for comparative purposes (Figure 2E). As previously reported, the Δ*psrA* pThy strain consistently maintained 1 $\log_{10}$ lower than that of Lp02 pThy ($p = 0.029$) (Graham *et al*., 2021). The mean growth profile of the Lp02 pVect-*dksA* strain showed a subtle increase of ~½ $\log_{10}$ over that of Lp02 pThy ($p = 0.007$); this enhancement could also be seen in the Δ*dksA* pVect-*dksA* complemented strain (Figure 2D; $p = 0.0247$). Likewise, we found that *in trans* expression of DksA in the Δ*psrA* pVect-*dksA* strain rescued the growth defect of Δ*psrA* strain, increasing growth by ~1 $\log_{10}$ to match that of Lp02 pThy strain ($p < 0.001$ versus Δ*psrA* pThy, not significant versus Lp02 pThy). Although this experiment did not generate large phenotypic differences, we found the tendency towards subtle phenotypes upon *in trans* expression of DksA to be noteworthy relative to the very strong phenotypes noted in the *dksA* mutant strains.

DksA is not required for intracellular growth in human U937-derived macrophages

Some *L. pneumophila* genes exhibit host specific requirements such that a subset are required only for growth in one host type, but not in another. Previous work showed that the human U937-derived macrophage infection model is more permissive to *L. pneumophila* regulatory mutant strains than *A. castellanii*, as exemplified by transcriptional regulator Δ*psrA* or Δ*cpxRA* TCS mutants (Tanner *et al.,* 2016; Graham *et al.,* 2021). DksA was previously shown to be dispensable for growth in primary murine bone marrow macrophages (Dalebroux *et al.,* 2010).

412 However, since the phenotype we observed for the Δ*dksA* strain in *A. castellanii* was different
413 from that reported by Dalebroux *et al*. (2010), we decided to ascertain the phenotype using the
414 human monocytic U937 cell-line as a representative mammalian cell model. Intracellular growth
415 kinetics were assessed for the same set of strains previously used in the *A. castellanii* infection
416 assays (Figure 2). As expected, Lp02 pThy grew well, increasing approximately 100-fold by the
417 72 h timepoint (Figure 3A), and Δ*dotA* pThy maintained a steady titre with no growth. In
418 comparison to that of Lp02 pThy, Δ*dksA* pThy and Δ*dksA* Δ*psrA* pThy showed similarly robust,
419 but offset growth profiles. Additionally, despite normalization of the inoculum by OD_{600}, these
420 two strains showed initial quantified titres lower than that of Lp02 pThy (Figure 3A). Only
421 Δ*dksA* Δ*psrA* pThy showed a significant deviation from Lp02 pThy ($p = 0.049$). The Δ*dksA*
422 pVect-*psrA* showed a similar profile to that of Lp02 pThy (Figure 3A), and did not show the
423 reduced starting titre, but the difference to Δ*dksA* pThy was not significant. No significant
424 change in phenotype was observed with the remaining set of strains featuring *in trans* DksA
425 expression, either by complementation (Δ*dksA* pVect-*dksA*), overexpression, (Lp02 pVect-*dksA*)
426 or in Δ*psrA* pVect-*dksA* (Figure 3B). The growth profiles of the *dksA1* pThy, *dks1* Δ*psrA* pThy,
427 or *dksA1* pVect-*psrA* were indistinguishable from Lp02 pThy (Figure 3C) and lacked even
428 variability in the initial uptake. Thus, these results verify that DksA is not required for, nor does
429 it enhance, intracellular growth in U937-derived macrophages.
430
431 ***In vitro* growth is impacted by DksA, PsrA and DksA1** The differences observed with the
432 intracellular growth kinetics of isogenic mutant strains with and without *in trans* gene expression
433 constructs in *A. castellanii* may be in part due to defects in the growth rates of the cells, rather
434 than solely virulence defects *in vivo*. To distinguish this possibility and more generally

435 characterize the *in vitro* growth characteristics of the strains, we tested the *in vitro* growth rates
436 of the strains in BYE broth at 37ºC over a 24-hour time period (Figure 4). While the growth
437 profiles of *dksA1* pThy and Lp02 pThy were similar to one another, both were distinct from the
438 growth profile of Δ*psrA* pThy which was significantly reduced in comparison to that of *dksA1*
439 pThy ($p = 0.0092$) and Lp02 pThy ($p = 0.0007$) (Figure 4A) with the latter comparison consistent
440 with our previous study (Graham *et al*., 2021). The growth profiles of Lp02 pThy, *dksA1* pVect-
441 *psrA*, and *dksA1* Δ*psrA* pThy were all similar to one another indicating that lack of PsrA, or
442 elevated levels of PsrA from *in trans* expression, did not affect the growth profile of the *dksA1*
443 (Figure 4B). Interestingly, the *in vitro* growth kinetics of Δ*dksA*-based strains featured growth
444 variability across replicates as manifested by the large error bars for hourly data points (Figures
445 4C and 4D). Despite this variability, the growth profile of Δ*dksA* pThy was not considered to be
446 significantly different from that of Lp02 pThy (Figure 4C). Notably, the growth variability
447 disappeared from the Δ*dksA* pVect-*dksA* growth profile suggesting this was a complementable
448 phenomenon (Figure 4C). *In trans* expression of *dksA1* (Δ*dksA* pVect-*dksA1*) significantly
449 reduced the growth profile in comparison to that of Lp02 pThy ($p = 0.0053$) indicating the
450 elevated levels of DksA1 compromised replicative growth (Figure 4C). As observed with *dksA1*
451 Δ*psrA* pThy (Figure 4B), the growth profile of Δ*dksA* Δ*psrA* pThy was similar to that of Lp02
452 pThy (Figure 4D) indicating the dispensability of PsrA. *In trans* expression of DksA in Lp02
453 (Lp02 pVect-*dksA*) did not alter the growth profile from that of Lp02 pThy (Figure 4E). While a
454 significant reduction was observed for the growth profile of Δ*psrA* pVect-*dksA* in comparison to
455 that of Lp02 pThy ($p = 0.0053$; Figure 4E), the difference was not due to *in trans* expression of
456 DksA as a similar difference was observed for Δ*psrA* pThy versus Lp02 pThy (Figure 4A). *In*
457 *trans* expression of PsrA did not reduce the growth variability phenotype of Δ*dksA* nor was the

458 growth profile significantly different from that of Lp02 pThy (Figure 4F). *In trans* expression of
459 DksA1 had no effect as the growth profiles of Lp02 pVect-*dksA1* and Lp02 pThy were similar
460 (Figure 4E).

461 The *in vitro* growth profile assays were repeated at 25°C, albeit over a 48-hour time
462 period to account for the slower growth rate, to mimic the incubation temperature of the *A.*
463 *castellanii* assays. The resultant growth profiles were mostly similar to those attained at 37°C,
464 with growth variability of Δ*dksA* pThy exacerbated at 25°C as indicated by data points with
465 widened error bars (Figure 5C). One notable difference was that the growth profile of Δ*dksA*
466 pVect-*dksA1* matched that of Lp02 pThy at 25°C (Figure 5D), versus the reduction at 37°C
467 (Figure 4C), suggesting that the slower growth rate and/or lower temperature accommodated the
468 dysfunctional nature of DskA1.

469 These findings together suggest that while strains lacking *dksA* featured more variability
470 in growth profiles, more so at 25°C then at 37°C, the *in vitro* growth assays (Figures 4 and 5)
471 illustrates that the observed *in vivo* growth defects are specific to *A. castellanii* (Figure 2), and
472 not due to poor growth of the bacterial cells themselves.

473

474 **DksA, and possibly PsrA, affects cell morphology** Throughout this study, it was noted that the
475 colony morphologies of Δ*dksA* and *dksA1* strains grown on BCYE agar plates differed
476 significantly from that of Lp02. In comparison to the opaque beige-white glossy colonies with
477 varied margins featured by Lp02, Δ*dksA* colonies were textured matte white with defined
478 margins, and *dksA1* colonies were smooth glossy white with defined margins. The phenotypes
479 were particularly evident when bacterial suspensions in broth were spotted onto BCYE agar
480 plates as were done in serial dilution assays in this study (Figure 6). The phenotype was fully

481 rescued by *in trans* expression of DksA for both Δ*dksA* and *dksA1* strains, whereas *in trans*
482 DksA1 expression only partially rescued the phenotype of the Δ*dksA* strain. The colony
483 morphology of the Δ*dksA* Δ*psrA* strain was similar to that of the Δ*dksA* strain, but not to the
484 Δ*psrA* strain which was similar to that of Lp02 indicating the sole influence of DksA. Finally, *in*
485 *trans* PsrA expression did not appear to alter colony morphology in all strain backgrounds
486 assessed (Lp02, Δ*dksA*, *dksA1,* Δ*psrA*) confirming that PsrA does not influence this phenotype.
487 We previously reported that PsrA promoted cell elongation when overexpressed *in trans*
488 (Graham *et al.,* 2021). Conversely, it was reported elsewhere that lack of DksA influenced cell
489 elongation (Dalebroux *et al*., 2010). To assess whether a genetic relationship between PsrA and
490 DksA was evident in cell structure morphology, and to further explore whether *dksA1* generated
491 a phenotype distinct from Δ*dksA*, bacteria in exponential growth phase (EP) and in stationary
492 phase (SP) were microscopically imaged (Figure 7) and analyzed for cell lengths (Figures 8A
493 and 8B). As a control, Lp02 pThy bacteria formed typical rods (mean length 3.6 µm) in EP, that
494 elongated into SP (mean length 5.8 µm). The Δ*dksA* pThy bacteria were notably elongated in EP
495 (mean length 6.2 µm) and, in SP, became extremely elongated into filamentous forms often of
496 sufficient length to often exceed the field of view, averaging 13.2 µm among measurable cells
497 (with the entire cell visible in one field of view). Likewise, the Δ*dksA* Δ*psrA* pThy bacteria were
498 also elongated in EP, and strongly filamentous in SP (mean lengths 5.4 µm and 17.1 µm,
499 respectively). Conversely, Δ*psrA* pThy bacteria were morphologically indistinguishable from
500 that of Lp02 pThy as previously observed (Graham *et al*, 2021). The filamentation of Δ*dksA*
501 pVect-*dksA* bacterial forms was rescued by *in trans* DksA expression as they were slightly, but
502 significantly shortened relative to Lp02 (2.9 µm and 4.7 µm in EP and SP phases, respectively).
503 Expression of DksA *in trans* in Δ*psrA* pVect-*dksA* and Lp02 pVect-*dksA* strains also resulted in

504 slightly, but significantly shorter cell lengths in comparison to those of Lp02 pThy and
505 comparable to Δ*dksA* pVect-*dksA* in both growth phases. *In trans* PsrA expression in Δ*dksA*
506 pVect-*psrA* did not strongly affect the bacterial cell lengths and elongation was still present (7.5
507 µm and 14.2 µm in EP and SP, respectively). These findings suggest that the shortening is
508 mediated by DksA independently of PsrA.

509 The bacterial forms of *dksA1* pThy, *dksA1 ΔpsrA* pThy, and *dksA1* pVect-*psrA* strain
510 were all slightly elongated relatively to Lp02 pThy in both EP (5.0 µm, 5.1 µm and 4.3 µm,
511 respectively) and SP (7.5 µm, 7.7 µm, and 7.8 µm, respectively), but were not considered
512 filamentous, and did not vary significantly from each other supporting the hypothesis that the
513 *dksA1* allele maintained partial function. Interestingly, the Δ*dksA* pVect-*dksA1* strain did not
514 show rescue of the elongation to resemble *dksA1* levels as might be expected (5.6 µm in EP, 12.3
515 µm in SP). To rule out the simple possibility of the two gene products conflicting in some way,
516 we tested the *dksA1* pVect-*dksA* (plasmid- and chromosomal based alleles reversed). The
517 bacterial forms of this strain appeared somewhat shortened relative to Lp02 pThy in SP only (4.2
518 µm) resembling the other *in trans* DksA expression strains, suggesting that relative protein
519 concentrations may drive the phenotype. Together, this indicates that the previously reported role
520 of PsrA is overshadowed by the more potent role of DksA, and that the DksA1 protein shows an
521 intermediate phenotype illustrating that DksA1 is a partially functional protein in these strains.
522

523 **DksA, or DksA1, is necessary for extended culturability in depleted media** Previously, the
524 insertional mutant Δ*dksA* strain was also noted to feature reduced recovery of culturable bacteria
525 after extended incubation in depleted media, which the authors referred to as "survival" (i.e.
526 culturability) (Dalebroux *et al.,* 2010). Over the course of this study, we noticed that the Δ*dksA*

527 mutants could not be consistently sub-cultured, or often failed to grow entirely, if taken from
528 BCYE agar plates grown more than three days. In view of this, we asked if this was a
529 consequence of previously observed culturability phenotype occurring in the Δ*dksA* strain, and
530 potentially the *dksA1* strains, and whether PsrA may also contribute. As this phenotype had not
531 been assessed in the prior PsrA study (Graham *et al.*, 2021), we decided to include Δ*psrA* pThy,
532 Δ*psrA* pVect-*psrA* and Lp02 pVect-*psrA* strains from Graham *et al.* (2021).
533 Over the time course, optical density values peaked comparably for all strains at 24 h,
534 and held steadily to the 96 h timepoint (Figure 9). Enumeration of titres for Lp02 pThy and
535 Δ*psrA* pThy were comparable to one another (Figure 9A). The titres for Δ*dksA* pThy (Figure 9C)
536 and Δ*dksA* Δ*psrA* pThy (Figure 9A) were significantly reduced by 72 h, and more so by the 96 h
537 for Δ*dksA* pThy (Figure 9C), noting that titre enumeration was not possible for Δ*dksA* Δ*psrA*
538 pThy at 96 h as no colonies were recovered in any replicate for this strain at that timepoint
539 (detection limit ~10^2 CFU/mL; Figure 9A). The reduced culturability phenotype was rescued by
540 *in trans* expression of DksA (Figure 9B) or DksA1 (Figure 9C), but not PsrA (Figure 9B). The
541 extended culturability of *dksA1* pThy strain was unaffected in comparison to Lp02 pThy, thereby
542 not requiring nor significantly benefiting from *in trans* expression of DksA or PsrA (Figure 9D).
543 The unaltered phenotype of the *dksA1* Δ*psrA* pThy in comparison to the *dksA1* pThy strain
544 further supports the observation that PsrA does not contribute to extended culturability (Figure
545 9E). Further, *in trans* expression of DksA in the Lp02 strain does not significantly improve
546 extended culturability (Figure 9F). Thus, in summary, PsrA plays no role in extended
547 culturability, while DksA is essential for the culturability of Lp02 in depleted media as reported
548 elsewhere previously (Dalebroux *et al.,* 2010). Notably, the hypomorph *dskA1* allele has retained
549 this essential function of promoting extended culturability.

550 **Pigmentation requires fully functional DksA, but not PsrA** *L. pneumophila* pigment is a
551 brown, melanin-like secreted protein that is released into the supernatant during the transition to
552 stationary phase under the control of the stringent response through RelA (Zusman *et al*., 2002;
553 Dalebroux *et al.*, 2010). Further, we observed hyperpigmentation of a subset of parental, isogenic
554 (Δ*psrA*, Δ*dksA*) and *dksA1* strains producing DksA *in trans* (Figure 10A). To ascertain whether
555 DksA1 and/or PsrA could contribute to this hyperpigmentation, we quantified the pigmentation
556 for each strain as done elsewhere (Wiater *et al.*, 1994; Dalebroux *et al.,* 2010) (Figure 10B).
557 Lp02 pThy strain developed moderate pigmentation (Abs_{550}/OD_{600} = ~0.20) that was
558 similarly achieved by Δ*psrA* pThy, Δ*psrA* pVect-*psrA*, and Lp02 pVect-*psrA* strains suggesting
559 that PsrA does not influence pigmentation (Figure 10B). This supposition is further borne out by
560 the significantly reduced pigmentation (Abs_{550}/OD_{600} = 0.10 - 0.12) featured by both of the
561 Δ*dksA* Δ*psrA* pThy and Δ*dksA* pThy strains. Significantly increased levels (i.e.
562 hyperpigmentation) was achieved by the Δ*dksA* pVect-*dksA* strain (Abs_{550}/OD_{600} = 0.36 - 0.38)
563 which exceeded that of Lp02 pThy likely due to *in trans* production of DksA (Figure 10B).
564 Indeed, the pigmentation phenotype was rescued by *in trans* DksA expression in the Δ*psrA*
565 strain, but not by *in trans* PsrA expression in the Δ*dksA* strain, clearly indicating that only DksA
566 positively influences pigmentation (Figure 10B). Pigmentation was also significantly and
567 equitably reduced (Abs_{550}/OD_{600} = 0.05 - 0.09) for the *dksA1* pThy and *dksA1* Δ*psrA* strains. As
568 the phenotype was not rescued by *in trans* PsrA expression in the *dksA1* pThy strain, this further
569 supports the lack of involvement in pigmentation by PsrA (Figure 10B). Surprisingly, the
570 hypomorph DksA1 could not rescue pigmentation in the Δ*dksA* strain, but pigmentation of *dksA1*
571 strain could be induced by *in trans* DksA expression. The *dksA1* pVect-*dksA* strain showed
572 delayed onset of hyperpigmentation such that only one of three replicates had fully pigmented by

573 30 h, with all replicates of this strain pigmented by 48 h (Figure 10A), but at 30 h the difference
574 was not statistically significant. These findings indicate that the ability of DksA1 to interact with
575 RNAP is impaired as suggested by structural modelling (Figures 1, 10B). Taken together, these
576 results indicate that DksA is sufficient to drive pigmentation independently of PsrA.
577
578 **Growth in long chain fatty acids is mediated by PsrA and DksA** The activation of the
579 biphasic switch is mediated in part by the response to fatty acid flux (Edwards *et al.,* 2009;
580 Dalebroux *et al.,* 2010). It was shown elsewhere that *in vitro* supplementation of short chain fatty
581 acids (SCFAs), such as propionic acid, will trigger the expression of TP traits (Edwards *et al.,*
582 2009). Further, the process of differentiation in response to excess SCFAs is mediated by DksA
583 (Dalebroux *et al.,* 2010). PsrA is also associated with differentiation though the precise role
584 remains to be elucidated (Graham *et al*., 2021). The *Pseudomonas* PsrA ortholog is a sensor of
585 long chain fatty acids (LCFAs) of which presence alleviates PsrA-mediated repression of the
586 *fadBA5* β-oxidation operon (Kang *et al*., 2008). To investigate where PsrA also responds to
587 LCFAs, Δ*psrA* strains with and without *in trans* gene expression constructs were grown in BYE
588 broth supplemented with the LCFA palmitic acid to ascertain impact on bacterial growth. In
589 comparison to Lp02, 2-fold growth inhibition of the Δ*psrA* pThy strain was observed which was
590 rescued by *in trans* PsrA expression strongly suggesting that PsrA responds to LCFAs (Figure
591 11A). Because chromosomal-based DksA expression is present in the Δ*psrA* pThy strain, we
592 next asked if DksA also responded to palmitic acid which could be amplified through *in trans*
593 DksA expression in the Δ*psrA* strain background. While it appears that growth of the Δ*psrA*
594 pVect-*dksA* strain improved in comparison to the Δ*psrA* pThy strain, it was not found to be
595 statistically significant (Figure 11A). Likewise, *in trans* DksA expression in Lp02 did not

596 significantly improve bacterial growth over that of Lp02 alone (Figure 11A). Conversely, *in*
597 *trans* DksA expression significantly improved bacterial growth over that of Lp02 (Figure 11A).
598 To further investigate the role of DksA, Δ*dksA*-based strains were also assessed. The Δ*dksA*
599 Δ*psrA* pThy strain had 2-fold growth inhibition in comparison to Lp02 (Figure 11B). Growth
600 inhibition of the Δ*dksA* pThy strain was not considered statistically different from that of Lp02
601 (Figure 11B). Surprisingly, *in trans* PsrA expression in the Δ*dksA* strain could not fully rescue
602 the growth inhibition phenotype. Taken together, these results suggest that while PsrA is largely
603 responsible for the response to LCFAs, DksA also contributes additively to this response lending
604 support to the overlapping roles observed for the two regulatory factors for some of the traits in
605 this study.
606
607
608
609
610
611
612
613
614
615
616
617
618

619 **Discussion**

620 The biphasic lifecycle of *L. pneumophila* is controlled by the convergence of multiple signals
621 into a sophisticated regulatory network that ultimately acts to induce TP differentiation. The
622 primary signals driving differentiation link to the nutritional status of the environment, mediated
623 largely by induction of the stringent-response and the associated downstream regulatory network
624 in association with RNAP-binding cofactor DksA, alternative sigma factor RpoS, two-
625 component systems and a subset of transcriptional regulators including PsrA (Fonseca and
626 Swanson, 2014; Oliva *et al*., 2018; Graham *et al*., 2024).

627 This study investigated a spontaneous *dksA1* mutation resulting in a truncated DksA1
628 protein featuring a deletion within its CC domain (Figure 1) (Perederina *et al,* 2004; Dalebroux
629 *et al.,* 2010). The intermediate phenotype observed in bacteria expressing DksA1 relative to
630 DksA can be explained by comparing their AlphaFold2 models to that of *E. coli* DksA bound to
631 RNAP (Figure 1) (Molodtsov *et al*., 2018). These models predict DksA1 to be physically
632 incapable of coordinating Mg^{2+} in the active site of RNAP due to the truncated loop in the CC
633 domain (Figure 1D, F). However, DksA1 is still predicted to overall form the core CC and GH
634 domains (Parshin *et al*., 2015; Molodtsov *et al*., 2018). This would hypothetically still allow
635 DksA1 to bind into the allosteric binding pocket of RNAP (Figure 1C, S2), thereby recruiting a
636 secondary ppGpp to RNAP. This would partially explain the variance in phenotype of *dksA1* as
637 an intermediary between the WT and knockout strain. Likewise, these structural predictions also
638 fit into the model of the interplay between GreA and DksA as allosteric inhibitors/activators of
639 RNAP competing for the same allosteric site (Parshin *et al*., 2015; Molodtsov *et al*., 2018).

640 DksA1 (i.e. Δ*dksA1* pThy strain) affected reduced intracellular growth in *A. castellanii*
641 protozoa indicating impaired function that was partially, but not fully, rescued by *in trans*

642 expression of *psrA* (Figure 2A). This surprising finding compelled us to use the DksA1
643 hypomorph to explore overlapping cellular functions of both regulators, inferring a subset of
644 gene targets jointly regulated by DksA and PsrA. To explore the possibilities that either DksA
645 and PsrA interact with each other, or act in parallel, Δ*dksA* pThy and Δ*dksA* Δ*psrA* pThy strains
646 were subsequently assessed for growth kinetics in *A. castellanii* protozoa (Figure 2B). The
647 Δ*dksA* pThy strain developed a more severely avirulent phenotype than the *dksA1* pThy strain,
648 and was rescued by *in trans* expression of *dksA* or *dksA1* (Figures 2B and 2C), but not by *psrA*
649 (Figure 2B). Notably, the avirulent phenotype of the Δ*dksA* pThy strain contrasts to a previous
650 study showing that a Δ*dksA* insertional mutant strain only exhibited reduced intracellular growth,
651 rather than avirulence, in *A. castellanii* (Dalebroux *et al.,* 2010). While the assays done by
652 Dalebroux *et al*. (2010) and in this study were done in a comparable manner, the discrepancy in
653 findings could be due to differing experimental conditions as the former conducted *A. castellanii*
654 infections at 37°C. Temperature-dependent phenotypes have been seen previously, for example,
655 with Δ*hfq* mutant strains, which only showed an intracellular kinetic defect in *A. castellanii* at
656 30°C, but not at 37°C (McNealy *et al.,* 2005). We undertook the *A. castellanii* infections at 25°C
657 and showed that the avirulent phenotype of the Δ*dksA* pThy strain was fully complemented by *in*
658 *trans* DksA expression (Δ*dksA* pVect-*dksA*) indicating that the phenotype was solely due to the
659 genetic deletion of *dksA*. Another possibility for the discrepancy is the possibility of different
660 deletion strategies causing polar effects. Sahr *et al* (2012) annotated *L. pneumophila* Paris strain
661 *dksA* in an operon with an uncharacterized alpha/beta hydrolase *lpp2286* encoded downstream
662 and Lp02-derivative strains are likely similar. However, both our study and that of Dalebroux *et*
663 *al* (2010) showed the respective Δ*dksA* mutant strains were complementable and thus, the
664 discrepancy is unlikely a polar effect. Additionally, *in trans* expression of DksA1 was sufficient

665 to compensate for lack of DksA indicating that the truncation did not impact essential function of
666 DksA. Lastly, expression of DksA enhanced and rescued intracellular growth in Lp02 and Δ*psrA*
667 strains, respectively. Thus, DksA can compensate for lack of PsrA, and PsrA can partially
668 compensate for the reduced activity of DksA1, but cannot compensate for the absence of DksA
669 intracellularly in *A. castellanii*. Taken together, the interplay of DksA and PsrA in regulating
670 their gene targets is not fully reciprocal, indicating that successful intracellular growth in *A.*
671 *castellanii* is largely driven by DksA with assistance from PsrA.

672 The requirement of DksA for intracellular growth is host specific. DksA was shown
673 elsewhere to be dispensable for growth in primary murine macrophages (Dalebroux *et al*., 2010)
674 and for human U937-derived human macrophages as shown in this study (Figure 3). Likewise,
675 the Δ*dksA* Δ*psrA* pThy strain was not impeded for intracellular growth in U937-derived
676 macrophages, a finding similar to that previously found with the Δ*psrA* strain (Graham *et al*.,
677 2021). *In trans* expression of DksA in the Lp02 strain background enhanced intracellular growth
678 in protozoa (Figure 2E), but with little overall impact in U937-derived macrophages (Figure 3B),
679 a trend also seen with overexpression of PsrA (Graham *et al*., 2021). This suggests that elevated
680 levels of either PsrA or DksA on an individual basis imbued a positive effect on replication in *A.*
681 *castellanii* which does not equate to a substantial phenotype in U937-derived macrophages.

682 To further delineate the distinct and overlapping roles of DksA and PsrA, *in vitro*
683 approaches were pursued to examine the growth kinetics and phenotypes characteristic of TP-
684 associated traits of *L. pneumophila*. The induction of regulatory mechanisms controlling the
685 transition switch from RP to TP are generally comparably induced *in vivo* (e.g. in protozoa) and
686 *in vitro* (Byrne and Swanson, 1998). In this view, *in vitro* kinetic assays were undertaken to
687 show the interactions between DksA and PsrA were largely growth temperature-independent

688 (Figures 4 and 5). Interestingly, *in trans* expression of DksA1 in the Δ*dksA* strain affected
689 reduced growth rate (Figure 4C) at 37°C, but not at 25°C (Figure 5D), illustrating that the
690 predicted compromised transcriptional efficiency DksA1 affects growth rates at higher
691 temperatures. This is further supported by the growth profile of Δ*dksA* pVect-*dksA1* which
692 resembled that of Lp02 in *A. castellanii* (Figure 2C). The slow *in vitro* growth phenotype did not
693 apply to the Lp02 pVect-*dksA1* strain bearing chromosomally-expressed DksA, inferring that
694 *dksA1* is not a dominant-negative allele (Figure 4F). The growth profiles of *in vitro* grown *dksA1*
695 pThy and *dksA1* pVect-*psrA* were similar to each other at both at 25°C (Figures 4A, 4B) and
696 37°C (Figures 5A, 5B), but not in protozoa where a two-$\log_{10}$ recovery was achieved through *in*
697 *trans* expression of PsrA inferring shared gene targets.

698 Other TP-associated phenotypes include cellular filamentation, culturability, and
699 pigmentation are mediated by DksA independently as previously reported (Dalebroux *et al.,*
700 2010). Lack of DksA resulted in unusual colony morphology (Figure 6) and filamentation,
701 particularly in stationary phase (Figures 7-8). Recently, DksA was ascertained to have a pivotal
702 role in cell division in *E. coli*. Binding of ppGpp to DksA/RNAP indirectly activates the
703 divisome complex component FtsZ to modulate cell length and division (Anderson *et al*., 2023).
704 The absence of either DksA or ppGpp promotes cell filamentation for different reasons. Lack of
705 DksA prevents activation of cell division by ppGpp resulting whereas lack of ppGpp causes
706 DksA to switch from an activator to an inhibitor of FtsZ. Thus, by orthologous function, it is
707 likely that DksA behaves in the same manner in *L. pneumophila*. The dramatically reduced
708 bacterial culturability of Δ*dksA* pThy strain (Figure 9) demonstrates the inability of the strain to
709 physiologically respond to nutrient deprivation and other stressors, which is consistent with the
710 importance of DksA to the stringent response. Biologically, PsrA does not contribute to this

711 phenotype as demonstrated by transcriptomic analyses that showed few stress-related genes
712 under PsrA regulation (Graham *et al*., 2021). Because variability in filamentation and
713 culturability affected by lack of DksA can impact optical density to titre ratios of stationary
714 phase bacteria, extreme care was taken in this study to ensure that Δ*dksA*-based strains were
715 recovered from ≤ 3-day-old BCYE-agar plates to minimize this variability for *in vitro* growth
716 curves and inoculum titre for *in vivo* kinetics. Lastly, pigmentation comprises a brown tyrosine-
717 based metabolite produced post-exponentially by *L. pneumophila* as an adaptation to
718 environmental stress, potentially serving for photoprotection, iron acquisition, or as a biocide to
719 enhance *L. pneumophila* competitiveness in biofilms (Steinert *et al.,* 1995; Chatfield and
720 Cianciotto, 2017; Levin *et al.,* 2019). As reported elsewhere, DksA is a major driver of pigment
721 production (Figure 10) (Dalebroux *et al.,* 2010). Thus, these traits, other than cell length, do not
722 seem measurably impacted by the cellular levels of PsrA, indicating that PsrA may impact
723 virulence specific pathways rather than cellular physiology.

724 Another phenotypic trait associated with TP differentiation is fatty acid flux which is
725 linked through SpoT-mediated stringent induction, with either DksA or ppGpp, sufficient to
726 arrest growth upon supplementation with SCFA (Edwards *et al.,* 2009; Dalebroux *et al.,* 2010).
727 Here, we show that like its ortholog in *Pseudomonas* spp., PsrA is responsive to fatty acids
728 suggesting a conserved functional role in sensing LCFA in the environment alongside SpoT.
729 Further, both DksA and PsrA must be present to ensure a proper LCFA response (Figure 11)
730 (Kang *et al.*, 2008). However, the precise mechanistic details of the PsrA-mediated response
731 remain undefined warranting further investigations.

732 In summary, this study explored the phenotypic roles of spontaneously mutated DksA1
733 and PsrA, and uncovered a synergistic genetic relationship between PsrA and DksA in terms of

734 virulence regulation. The bacterial response to LCFA suggests a novel regulatory link to the
735 stringent response pathway, further solidifying the mechanistic importance of both DksA and
736 PsrA as contributing regulators of the biphasic lifestyle of *L. pneumophila.* Because only the
737 predicted, rather than the functional, basis of the *dksA1* phenotype has been derived, these results
738 cannot distinguish the distinct effects of ppGpp recruitment and competitive sequestration of
739 RNAP from GreA. With these limitations in mind, our findings suggest that PsrA seems to
740 redundantly act as a bypass for DksA in virulence but has little impact on other processes,
741 suggesting a more targeted mechanism. The overlapping phenotypes presented in this study are
742 consistent with the two distinct mechanisms by which DksA and PsrA act, and thus the following
743 model is proposed based on a scenario in which a promoter is repressed by either DksA or PsrA
744 (Figure 12). Absence of DksA would permit GreA to act as the sole secondary channel binding
745 protein, thereby allowing increased efficiency in transcription initiation, and should there be
746 elevated levels of PsrA, it would result in increased promoter blockage providing compensatory
747 repression. Absence of PsrA would leave the promoter more accessible for RNAP, but this could
748 be counteracted should there be elevated levels of DksA resulting in reduced transcriptional
749 efficiency. Alternatively, a promoter not subject to PsrA-mediated influence would be exempt
750 from the compensatory effects, and thus be wholly dependent on the dynamics between GreA
751 and DksA. Nevertheless, the proposed co-regulator duality could explain why transcriptomic
752 analyses did not overtly reveal a large number of PsrA-regulated targets (Graham *et al*., 2021).
753 Thus, future transcriptomic studies will include the Δ*dksA* Δ*psrA* strain to compare against data
754 obtained for individual Δ*psrA* and Δ*dksA* strains to discern distinct and overlapping roles. These
755 studies could also be expanded to include the $ppGpp^0$ (Δ*relA* Δ*spoT*) strain to further explore the
756 interface with PsrA and ppGpp in relation to the link between PsrA and the fatty acid response.

Acknowledgements

We thank M. Swanson (University of Michigan) for the kind gift of pBH6119 and Lp02, J. Vogel (Washington University) for the kind gift of pSR47s and pJB908, R. R. Isberg (Tufts University) for the kind gift of Lp03. This work was supported by Natural Sciences and Engineering Research Council (NSERC) Discovery Grant funds awarded to A.K.C.B (RGPIN-2019-05490), T.dK. (RPIN-2017-04970) and G.P. (RGPIN-2018-04968), and Canadian Foundation for Innovation (CFI) Grant funds to A.K.C.B. Research personnel were supported by University of Manitoba Faculty of Graduate Studies (C.G., T.M, T.P., J.B.), Research Manitoba Master's Studentship Award (T.P.), and NSERC CGS Masters (T.M, A.G.) and Doctoral (T.M., T.P, A.G.).

780 **References**

781 Aberg, A., Shingler, V. and Balsalobre, C. (2008) Regulation of the *fimB* promoter: a case of
782 differential regulation by ppGpp and DksA *in vivo*. *Mol Microbiol*. **67**:1223-1241.

783 Aberg, A., Fernández-Vázquez, J., Cabrer-Panes, J.D., Sánchez, A. and Balsalobre, C. (2009).
784 Similar and divergent effects of ppGpp and DksA deficiencies on transcription in *Escherichia*
785 *coli. J Bacteriol.* **191**: 3226-3236.

786 Abu-Zant, A., Asare, R., Graham, J.E. and Abu Kwaik, Y. (2006. Role for RpoS but not RelA of
787 *Legionella pneumophila* in modulation of phagosome biogenesis and adaptation to the
788 phagosomal microenvironment. *Infect Immun.* **74**:3021-3026.

789 Al-Khodor, S., Kalachikov, S., Morozova, I., Price, C. T. and Abu Kwaik, Y. (2009) The
790 PmrA/PmrB two-component system of *Legionella pneumophila* is a global regulator required for
791 intracellular replication within macrophages and protozoa. *Infect Immun*. **77**:374-386.

792 Anderson, S.E., Vadia, S.E., McKelvy, J. and Levin, P.A. (2023) The transcription factor DksA
793 exerts opposing effects on cell division depending on the presence of ppGpp. *mBio*
794 **14**(6):e0242523.

795 Ashkenazy, H., Abadi, S., Martz, E., Chay, O., Mayrose, I., Pupko, T. and Ben-Tal, N. (2016)
796 ConSurf 2016: an improved methodology to estimate and visualize evolutionary conservation in
797 macromolecules. *Nucleic Acids Res* 8;**44**(W1):W344-50.

798 Bachman, M.A. and Swanson**,** M.S. (2001) RpoS co-operates with other factors to induce
799 *Legionella pneumophila* virulence in the stationary phase. *Mol Microbiol.* **40**:1201-1214.

800 Burstein, D., Amaro, F., Zusman, T., Lifshitz, Z., Cohen, O., Gilbert, J.A., Pupko, T., Shuman,
801 H.A. and Segal, G. (2016) Genomic analysis of 38 *Legionella* species identifies large and diverse
802 effector repertoires. *Nat Genet.* **48**:167-175.

803 Chatfield, C.H. and Cianciotto, N.P. (2007). The secreted pyomelanin pigment of *Legionella*
804 *pneumophila* confers ferric reductase activity. *Infect Immun*. **75**: 4062-4070.

805 Chatterji, D., Fujita, N. and Ishihama, A. (1998) The mediator for stringent control, ppGpp,
806 binds to the beta-subunit of *Escherichia coli* RNA polymerase. *Genes Cells* **3**:279-287.

807 Dalebroux, Z.D., Yagi, B.F., Sahr, T., Buchrieser, C. and Swanson, M.S. (2010) Distinct roles of
808 ppGpp and DksA in *Legionella pneumophila* differentiation. *Mol Microbiol.* **6**:200-219.

809 Edwards, R.L., Dalebroux, Z.D. and Swanson, M.S. (2009) *Legionella pneumophila* couples
810 fatty acid flux to microbial differentiation and virulence. *Mol Microbiol.* **71**:1190-1204.

811 Feldheim Y.S., Zusman T., Speiser Y. and Segal G. (2016) The *Legionella pneumophila* CpxRA
812 two-component regulatory system: new insights into CpxR's function as a dual regulator and its
813 connection to the effectors regulatory network. *Mol Microbiol.* **99**:1059-1079.

814 Finsel, I. and Hilbi, H. (2015) Formation of a pathogen vacuole according to *Legionella*
815 *pneumophila*: how to kill one bird with many stones. *Cell Microbiol*. **17**:935-950.

816 Fonseca, M.V. and Swanson, M.S. (2014) Nutrient salvaging and metabolism by the intracellular
817 pathogen *Legionella pneumophila*. *Front Cell Infect Microbiol.* **4**:12.

818 Gomez-Valero, L., Rusniok, C., Carson, D., Mondino, S., Pérez-Cobas, A.E., Rolando, M.,
819 Pasricha, S., Reuter, S., Demirtas, J., Crumbach, J., Descorps-Declere, S., Hartland, E.L.,

820 Jarraud, S., Dougan, G., Schroeder, G.N., Frankel, G. and Buchrieser, C. (2019) More than
821 18,000 effectors in the *Legionella* genus genome provide multiple, independent combinations for
822 replication in human cells. *Proc Natl Acad Sci U S A.* **116**:2265-2273.

823 Gourse, R.L., Chen, A.Y., Gopalkrishnan, S., Sanchez-Vazquez, P., Myers, A. and Ross, W.
824 (2018) Transcriptional Responses to ppGpp and DksA. *Annu Rev Microbiol.* **72**:163-184.

825 Graham, C.I., Patel, P.G., Tanner, J.R., Hellinga, J., MacMartin, T.L., Hausner, G. and
826 Brassinga, A.K.C. (2021) Autorepressor PsrA is required for optimal *Legionella pneumophila*
827 growth in *Acanthamoeba castellanii* protozoa. *Mol Microbiol*. **116**:624-647.

828 Graham, C.I., MacMartin, T.L., de Kievit, T.R. and Brassinga, A.K.C. (2024) Molecular
829 regulation of virulence in *Legionella pneumophila*. *Mol Microbiol*. **121**:167-195.

830 Gummesson, B., Lovmar, M. and Nyström, T. (2013) A proximal promoter element required for
831 positive transcriptional control by guanosine tetraphosphate and DksA protein during the
832 stringent response. *J Biol Chem.* **288**:21055–21064.

833 Hales, L.M. and Shuman, H.A. (1999) The *Legionella pneumophila rpoS* gene is required for
834 growth *within Acanthamoeba castellanii*. *J Bacteriol.* **181**:4879-4889.

835 Hammer, B.K., Tateda, E.S. and Swanson, M.S. (2002) A two-component regulator induces the
836 transmission phenotype of stationary-phase *Legionella pneumophila. Mol Microbiol.* **44**:107-
837 118.

838 Häuslein, I., Sahr, T., Escoll, P., Klausner, N., Eisenreich, W. and Buchrieser, C. (2017)
839 *Legionella pneumophila* CsrA regulates a metabolic switch from amino acid to glycerolipid
840 metabolism. *Open Biology* **7**:170149.

841 Hovel-Miner, G., Pampou, S., Faucher, S.P., Clarke, M., Morozova, I., Morozov, P., Russo, J.J.,
842 Shuman, H.A. and Kalachikov, S. (2009) SigmaS controls multiple pathways associated with
843 intracellular multiplication of *Legionella pneumophila. J Bacteriol.* **191**:2461-2473.

844 Isberg, R.R., O'Connor, T.J. and Heidtman, M. (2009) The *Legionella pneumophila* replication
845 vacuole: making a cozy niche inside host cells. *Nat Rev Microbiol.* **7**:13-24.

846 Jumper, J., Evans, R., Pritzel, A., Green, T., Figurnov, M., Ronneberger, O., Tunyasuvunakool,
847 K., Bates, R., Žídek, A., Potapenko, A., Bridgland, A., Meyer, C., Kohl, S.A.A., Ballard, A.J.,
848 Cowie, A., Romera-Paredes, B., Nikolov, S., Jain, R., Adler, J., Back, T., Petersen, S., Reiman,
849 D., Clancy, E., Zielinski, M., Steinegger, M., Pacholska, M., Berghammer, T., Bodenstein, S.,
850 Silver, D., Vinyals, O., Senior, A.W., Kavukcuoglu, K., Kohli, P. and Hassabis, D. (2021)
851 Highly accurate protein structure prediction with AlphaFold. *Nature* **596**(7873):583-589.

852 Kagan, J.C. and Roy, C.R. (2002) *Legionella* phagosomes intercept vesicular traffic from
853 endoplasmic reticulum exit sites. *Nat Cell Biol.* **4**:945-954.

854 Kang, Y., Nguyen, D.T., Son, M.S. and Hoang, T.T. (2008) The *Pseudomonas aeruginosa* PsrA
855 responds to long-chain fatty acid signals to regulate the *fadBA5* beta-oxidation operon.
856 *Microbiology* **154**:1584-1598.

857 Landau, M., Mayrose, I., Rosenberg, Y., Glaser, F., Martz, E., Pupko, T. and Ben-Tal, N. (2005)
858 ConSurf 2005: the projection of evolutionary conservation scores of residues on protein
859 structures. *Nucleic Acids Res* **33**(Web Server issue):W299-302.

860 Lemke, J.J., Sanchez-Vazquez, P., Burgos, H.L., Hedberg, G., Ross, W. and Gourse, R.L. Direct
861 regulation of *Escherichia coli* ribosomal protein promoters by the transcription factors ppGpp
862 and DksA. *Proc Natl Acad Sci USA.* **108**(14):5712-7.

863 Levin, T.C., Goldspiel, B.P., Malik, H.S. (2019). Density-dependent resistance protects
864 *Legionella pneumophila* from its own antimicrobial metabolite, HGA. *Elife.* **8**: e46086.

865 McNealy, T.L., Forsbach-Birk, V., Shi, C. and Marre, R. (2005) The Hfq homolog in *Legionella*
866 *pneumophila* demonstrates regulation by LetA and RpoS and interacts with the global regulator
867 CsrA. *J Bacteriol.* **187**:1527-1532.

868 Magnusson, L.U., Gummesson, B., Joksimović, P., Farewell, A. and Nyström, T. (2007)
869 Identical, independent, and opposing roles of ppGpp and DksA in *Escherichia coli. J Bacteriol.*
870 **189**:5193-5202.

871 Molodtsov, V., Sineva, E., Zhang, L., Huang, X., Cashel, M., Ades, S.E. and Murakami, K.S.
872 (2018) Allosteric Effector ppGpp Potentiates the Inhibition of Transcript Initiation by DksA. *Mol*
873 *Cell* **69**(5):828-839.e5.

874 Molofsky, A.B. and Swanson, M.S. (2004) Differentiate to thrive: lessons from the *Legionella*
875 *pneumophila* life cycle. *Mol Microbiol.* **53**:29-40.

876 Mondino, S., Schmidt, S. and Buchrieser, C. (2020) Molecular mimicry: a paradigm of host-
877 microbe coevolution illustrated by *Legionella*. *mBio* **11**:e01201-20.

878 Morash, M.G., Brassinga, A.K., Warthan, M., Gourabathini, P., Garduño, R.A., Goodman, S.D.
879 and Hoffman, P.S. (2009) Reciprocal expression of integration host factor and HU in the
880 developmental cycle and infectivity of *Legionella pneumophila*. *Appl Environ Microbiol.*
881 **75**:1826-1837.

882 Myers, A.R., Thistle, D.P., Ross, W. and Gourse, R.L. (2020) Guanosine Tetraphosphate Has a
883 Similar Affinity for Each of Its Two Binding Sites on *Escherichia coli* RNA Polymerase. *Front*
884 *Microbiol* **11**:587098.

885 Nevo, O., Zusman, T., Rasis, M., Lifshitz, Z. and Segal, G. (2014) Identification of *Legionella*
886 *pneumophila* effectors regulated by the LetAS-RsmYZ-CsrA regulatory cascade, many of which
887 modulate vesicular trafficking. *J Bacteriol.* **196**:681-692.

888 Newton, H.J., Ang, D.K., van Driel, I.R. and Hartland, E.L. (2010) Molecular pathogenesis of
889 infections caused by *Legionella pneumophila. Clin Microbiol Rev.* **23**:274-298.

890 Oliva, G., Sahr, T. and Buchrieser, C. (2018) The life cycle of *L. pneumophila*: cellular
891 differentiation is linked to virulence and metabolism. *Front Cell Infect Microbiol.* **8**:3.

892 Parshin, A., Shiver, A.L., Lee, J., Ozerova, M., Schneidman-Duhovny, D., Gross, C.A. and
893 Borukhov, S. (2015) DksA regulates RNA polymerase in *Escherichia coli* through a network of
894 interactions in the secondary channel that includes Sequence Insertion 1. *Proc Natl Acad Sci U S*
895 *A* **112**(50):E6862-71.

896 Perederina, A., Svetlov, A., Vassylyeva, M., Tahirov, T., Yokoyama, S., Artsimovitch, I. and
897 Vassylyev, D. (2004). Regulation through the secondary channel-structural framework for
898 ppGpp-DksA synergism during transcription. *Cell* **118**:297-309.

899 Personnic, N., Striednig, B. and Hilbi, H. (2018) *Legionella* quorum sensing and its role in
900 pathogen-host interactions. *Curr Opin Microbiol.* **41**:29-35.

901 Pettersen, E.F., Goddard, T.D., Huang, C.C., Meng, E.C., Couch, G.S., Croll, T.I., Morris, J.H.
902 and Ferrin, T.E. (2021) UCSF ChimeraX: Structure visualization for researchers, educators, and
903 developers. *Protein Sci.* **30**(1):70-82.

904 Pitre, C.A.J., Tanner, J.R., Patel, P. and Brassinga, A.K.C. (2013) Regulatory control of
905 temporally expressed integration host factor (IHF) in *Legionella pneumophila. Microbiology*
906 **159**:475-492.

907 Potrykus, K. and Cashel, M. (2008) (p)ppGpp: still magical? *Annu Rev Microbiol*. **62**:35-51.

908 Rasis, M. and Segal, G. (2009) The LetA-RsmYZ-CsrA regulatory cascade, together with RpoS
909 and PmrA, post-transcriptionally regulates stationary phase activation of *Legionella pneumophila*
910 Icm/Dot effectors. *Mol Microbiol.* **72**:995-1010.

911 Robertson, P., Abdelhady, H. and Garduño, R.A. (2014) The many forms of a pleomorphic
912 bacterial pathogen-the developmental network of *Legionella pneumophila*. *Front Microbiol*.
913 **5**:670.

914 Ross, W., Vrentas, C.E., Sanchez-Vazquez, P., Gaal, T. and Gourse, R.L. (2013) The magic spot:
915 a ppGpp binding site on *E. coli* RNA polymerase responsible for regulation of transcription
916 initiation. *Mol Cell* **50**(3):420-9.

917 Ross, W., Sanchez-Vazquez, P., Chen, A.Y., Lee, J.H., Burgos, H.L. and Gourse, R.L. (2016)
918 ppGpp Binding to a Site at the RNAP-DksA Interface Accounts for Its Dramatic Effects on
919 Transcription Initiation during the Stringent Response. *Mol Cell* **62**(6):811-823.

920 Rowbotham, T.J. (1986) Current views on the relationships between amoebae, legionellae and
921 man. *Isr J Med Sci*. **22**:678-689.

922 Sahr, T., Bruggemann, H., Jules, M., Lomma, M., Albert-Weissenberger, C., Cazalet, C. and
923 Buchrieser, C. (2009) Two small ncRNAs jointly govern virulence and transmission in
924 *Legionella pneumophila. Mol Microbiol.* **72**:741-762.

925 Sahr, T., Rusniok, C., Dervins-Ravault, D. Sismeiro, O., Coppée, J.Y. and Buchrieser, C. (2012)
926 Deep sequencing defines the transcriptional map of *L. pneumophila* and identifies growth phase-
927 dependent regulated ncRNAs implicated in virulence. *RNA Biol*. **9**:503-19.

928 Sahr, T., Rusniok, C., Impens, F., Oliva, G., Sismeiro, O., Coppée, J.Y. and Buchrieser, C.
929 (2017) The *Legionella pneumophila* genome evolved to accommodate multiple regulatory
930 mechanisms controlled by the CsrA-system. *PLoS Genet.* **13**:e1006629.

931 Schell, U., Kessler, A. and Hilbi, H. (2014) Phosphorylation signalling through the *Legionella*
932 quorum sensing histidine kinases LqsS and LqsT converges on the response regulator LqsR. *Mol*
933 *Microbiol.* **92**:1039-1055.

934 Skolnick, J., Gao, M., Zhou, H. and Singh, S. (2021) AlphaFold 2: Why It Works and Its
935 Implications for Understanding the Relationships of Protein Sequence, Structure, and Function. *J*
936 *Chem Inf Model* **61**(10):4827-4831.

937 Steinert, M., Engelhard, H., Flugel, M., Wintermeyer, E. and Hacker J. (1995). The Lly protein
938 protects *Legionella pneumophila* from light but does not directly influence its intracellular
939 survival in *Hartmannella vermiformis*. *Appl Environ Microbiol.* **61**: 2428-2430.

940 Steinert, M., Hentschel, U. and Hacker, J. (2002) *Legionella pneumophila*: an aquatic microbe
941 goes astray. *FEMS Microbiol Rev*. **26**:149-162.

942 Tanner, J.R., Li, L., Faucher, S.P. and Brassinga, A.K. (2016) The CpxRA two-component
943 system contributes to *Legionella pneumophila* virulence. *Mol Microbiol.* **100**:1017-1038.

944 Tanner, J.R., Patel, P.G., Hellinga, J.R., Donald, L.J., Jimenez, C., LeBlanc, J.J. and Brassinga,
945 A.K.C. (2017) *Legionella pneumophila* OxyR Is a redundant transcriptional regulator that
946 contributes to expression control of the two-component CpxRA system. *J Bacteriol.* **199**:e00690-
947 16.

948 Tiaden, A., Spirig, T., Weber, S.S., Brüggemann, H., Bosshard, R., Buchrieser, C. and Hilbi, H.
949 (2007) The *Legionella pneumophila* response regulator LqsR promotes host cell interactions as
950 an element of the virulence regulatory network controlled by RpoS and LetA. *Cell Microbiol.*
951 **9**:2903-2920.

952 Tiaden, A., Spirig, T., Carranza, P., Brüggemann, H., Riedel, K., Eberl, L., Buchrieser, C. and
953 Hilbi, H. (2008) Synergistic contribution of the *Legionella pneumophila lqs* genes to pathogen-
954 host interactions. *J Bacteriol.* **190**:7532-7547.

955 Tilney, L.G., Harb, O.S., Connelly, P.S., Robinson, C.G. and Roy, C.R. (2001) How the parasitic
956 bacterium *Legionella pneumophila* modifies its phagosome and transforms it into rough ER:
957 implications for conversion of plasma membrane to the ER membrane. *J Cell Sci.* **114**:4637-
958 4650.

959 Travis, B.A. and Schumacher, M.A. (2022) Diverse molecular mechanisms of transcription
960 regulation by the bacterial alarmone ppGpp. *Mol Microbiol* **117**(2):252-260.

961 Vinella, D., Potrykus, K., Murphy, H. and Cashel, M. (2012) Effects on growth by changes of
962 the balance between GreA, GreB, and DksA suggest mutual competition and functional
963 redundancy in *Escherichia coli. J Bacteriol.* **194**:261–273.

964 Wiater, L.A., Sadosky, A.B. and Shuman, H.A. (1994) Mutagenesis of *Legionella pneumophila*
965 using Tn*903* dll*lacZ*: identification of a growth-phase-regulated pigmentation gene. *Mol*
966 *Microbiol*. **11**:641-653.

967 Zusman, T., Gal-Mor, O. and Segal, G. (2002) Characterization of a *Legionella pneumophila*
968 *relA* insertion mutant and toles of RelA and RpoS in virulence gene expression. *J Bacteriol.*
969 **184**:67-75.

970 Zusman, T., Aloni, G., Halperin, E., Kotzer, H., Degtyar, E., Feldman, M., Segal, G. (2007) The
971 response regulator PmrA is a major regulator of the *icm/dot* Type IV secretion system in
972 *Legionella pneumophila* and *Coxiella burnetii*. *Mol Microbiol.* **63**:1508-1523.

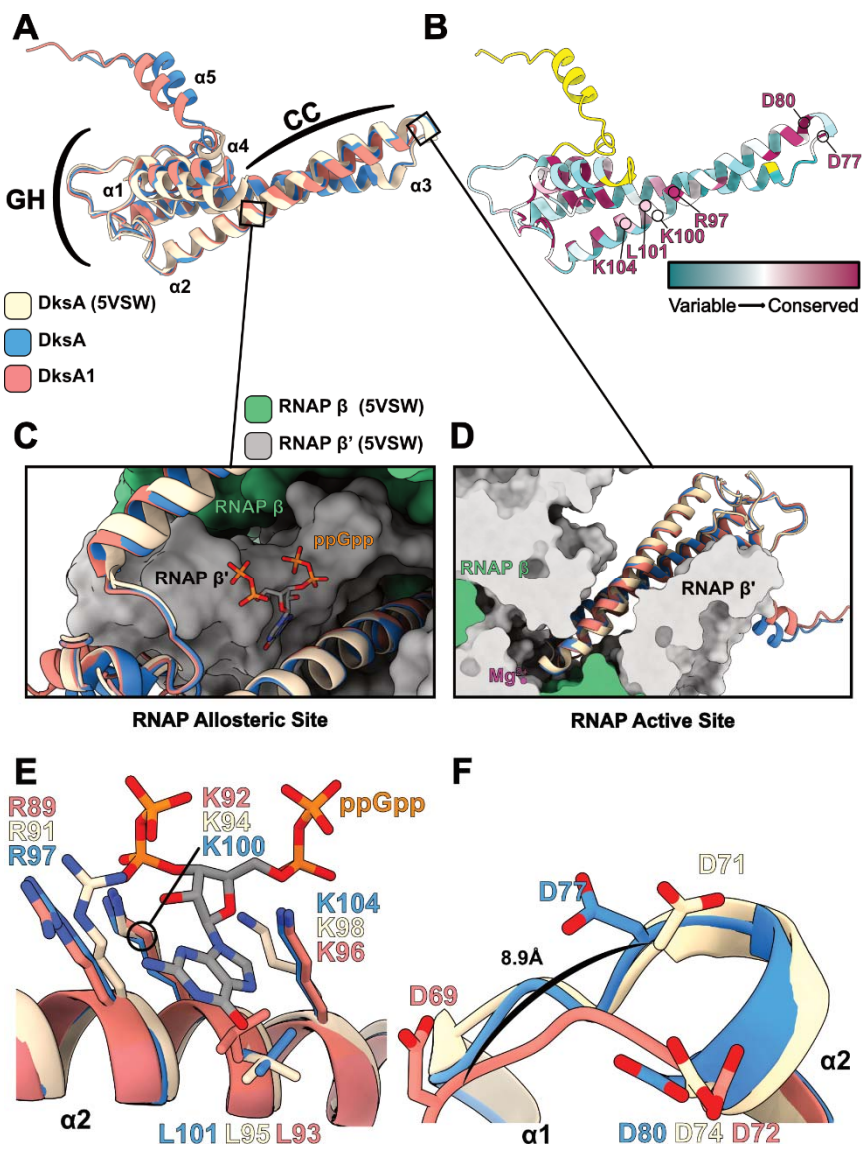

Figure 1: Structural comparison of DksA and DksA1 AlphaFold models. (A) Structural overlay of DksA (PDB ID: 5VSW) with both Lp02 DksA and DksA1 as modeled by AlphaFold. (B) Residue conservation of Lp02 DskA as plotted by the server Consurf (Landau *et al*., 2005; Ashkenazy *et al*., 2016). Yellow indicates insufficient information in the multisequence alignment. Indicated on the structure are conserved residues important for binding ppGpp and allostery with RNAP (R97 to K104), in addition to contact with the active site (D77-D80). (C) Binding of DksA with the RNAP allosteric site. A DksA:RNAP experimental structure (PDB ID: 5VSW) and aligned AlphaFold models are shown as cartoons, whereas RNAP is drawn as a molecular surface. The structure of ppGpp bound in the complex is also shown. (D) Slice view of DksA showing the contact point of residues D80 and D77 with magnesium in the RNAP active site. (D) Interactions of DksA variants with ppGpp in the RNAP allosteric site are shown and not disturbed by the truncation in DksA1. (E) Interactions of DksA variants with magnesium in the active site of RNAP are shown. AlphaFold predicts the truncation in DksA1 drastically moves the position of a critical aspartate residue (D69/71/77).

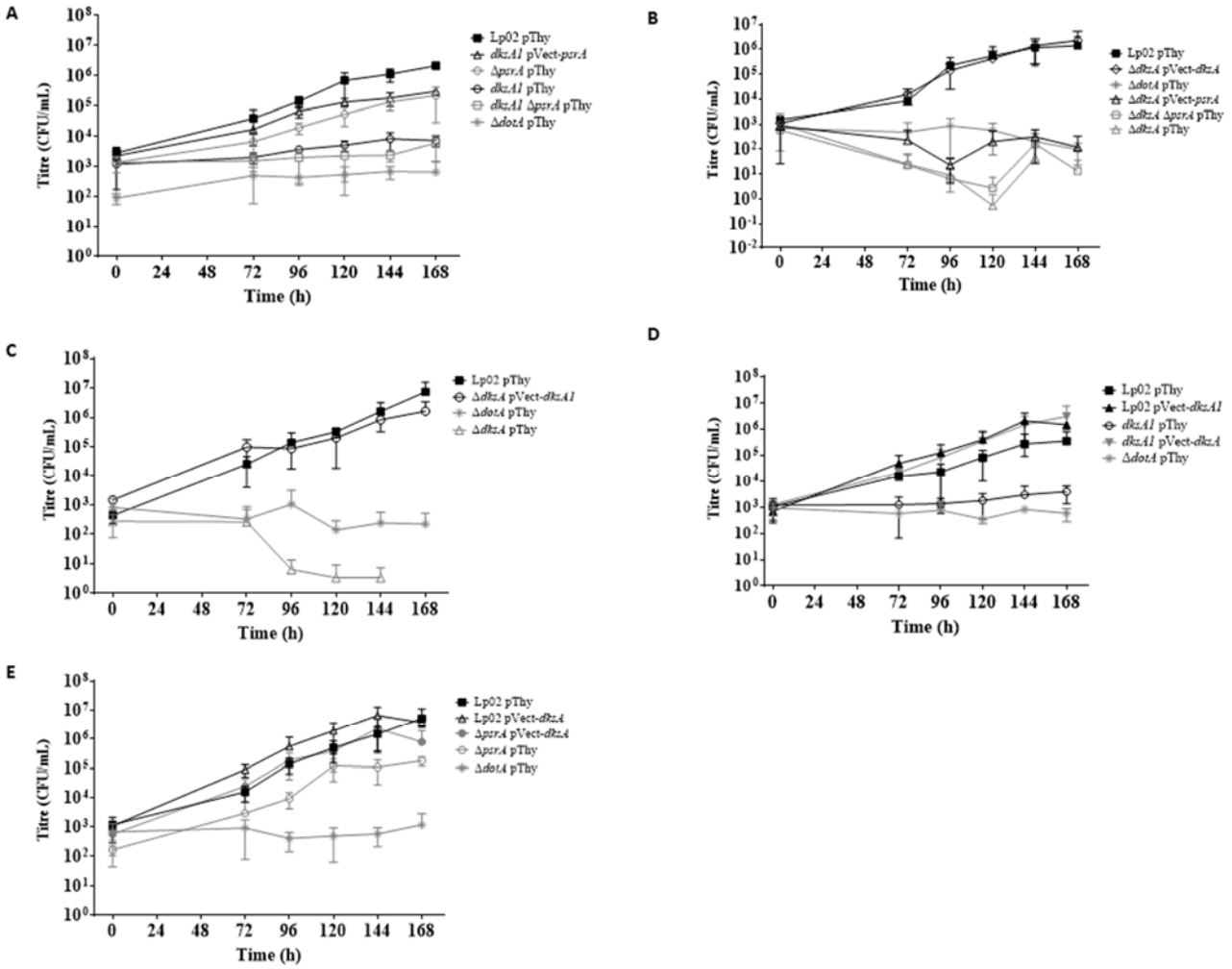

Figure 2: Synergistic impacts of DksA, DksA1, and PsrA on virulence of *L. pneumophila* in the *A. castellanii* protozoa. Intracellular growth kinetics of *L. pneumophila* strains in *A. castellanii* protozoa at 25ºC. Strains tested were parental Lp02 and avirulent Δ*dotA* along with isogenic strains featuring single or combinatorial genetic mutations (Δ*psrA*, Δ*dksA*, *dksA1*) with or without *in trans* expression of *psrA, dksA* or *dksA1*. Error bars represent SD across mean of three biological replicates, with two technical replicates each. Samples below detection limit (~10 CFU/mL) were recorded as zero and omitted from graph if they lacked countable colonies across all replicates.

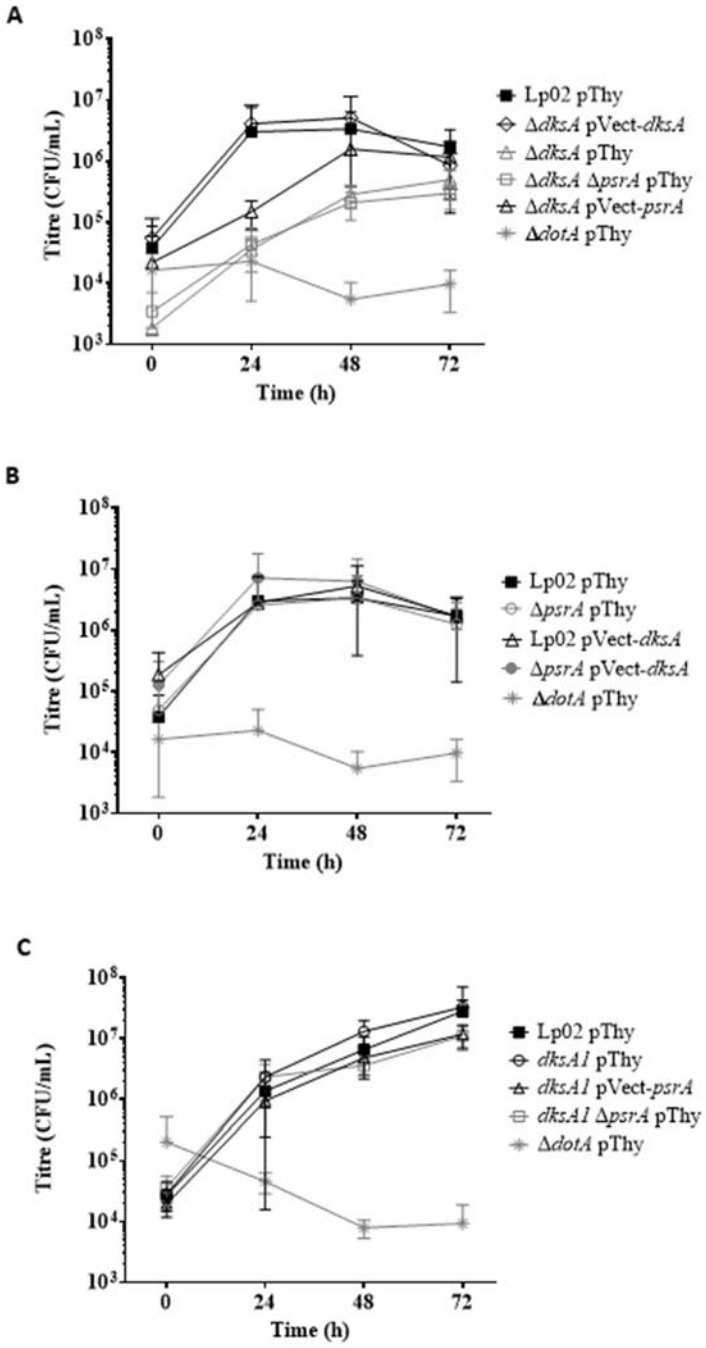

Figure 3: DksA is dispensable for growth in human macrophages. Intracellular growth kinetics of *L. pneumophila* strains in U937-derived macrophages at 37°C. Strains tested were parental Lp02 and avirulent Δ*dotA* along with isogenic strains featuring single or combinatorial genetic mutations (Δ*psrA*, Δ*dksA*, *dksA1*) with or without *in trans* expression of *psrA, dksA* or *dksA1*. Error bars represent SD across mean of three biological experiments with two technical replicates each. Experiments in panels A-C were conducted concurrently, but presented separately for clarity.

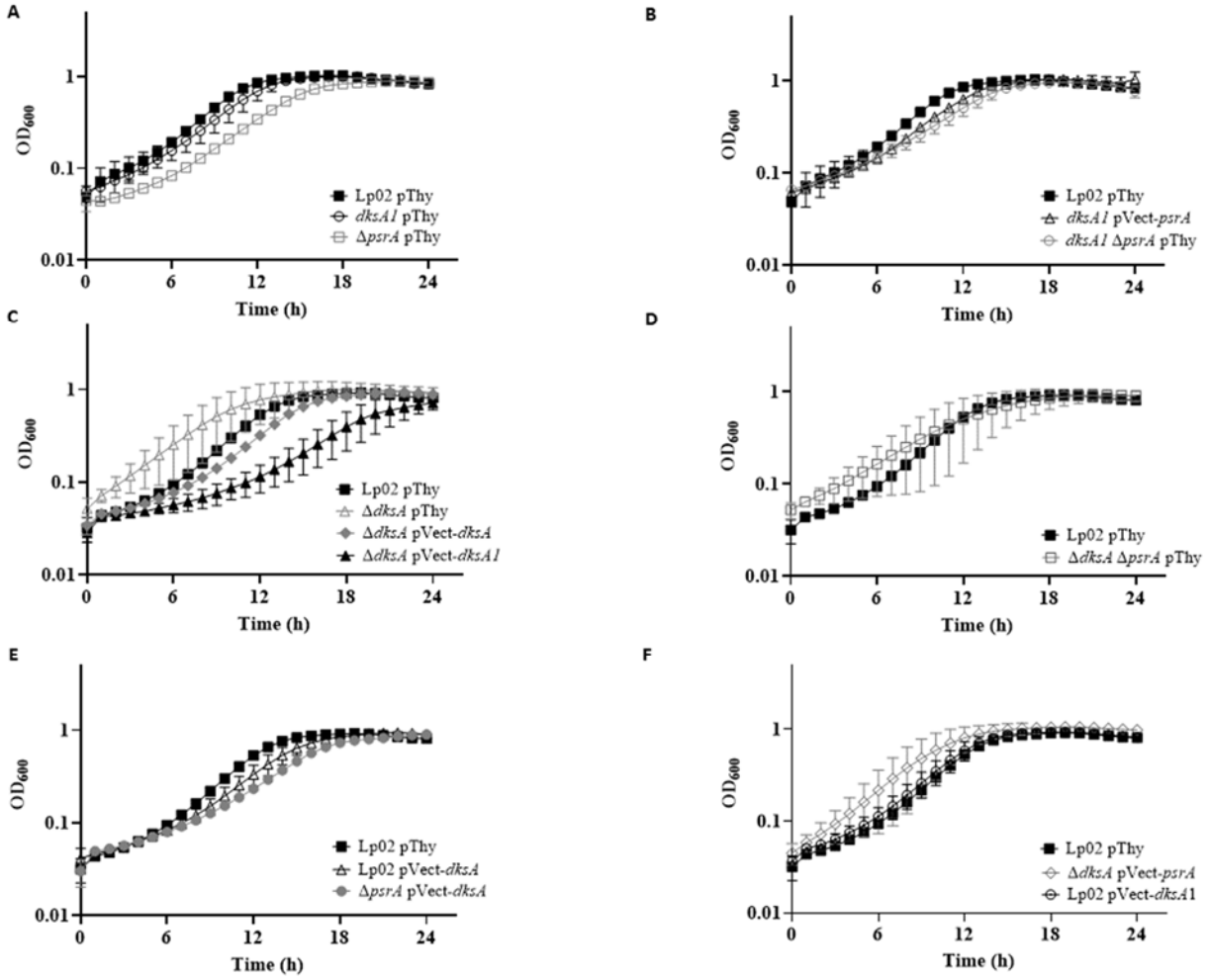

Figure 4: *L. pneumophila in vitro* growth at 37°C is impacted by DksA, PsrA and DksA1. *In vitro* growth kinetics of parental Lp02 and isogenic strains featuring single or combinatorial genetic mutations (Δ*psrA*, Δ*dksA*, *dksA1*) with and without *in trans* expression of *psrA, dksA* or *dksA1* genes. Plate-grown bacteria were suspended in BYE broth and normalized to initial OD_{600} = 0.15, and growth at 37°C was monitored for OD_{600} hourly for 24 h. Graphs in panels A-F were experiments conducted concurrently, but presented separately for clarity. Error bars are SD across mean of three independent biological replicates with three technical replicates each.

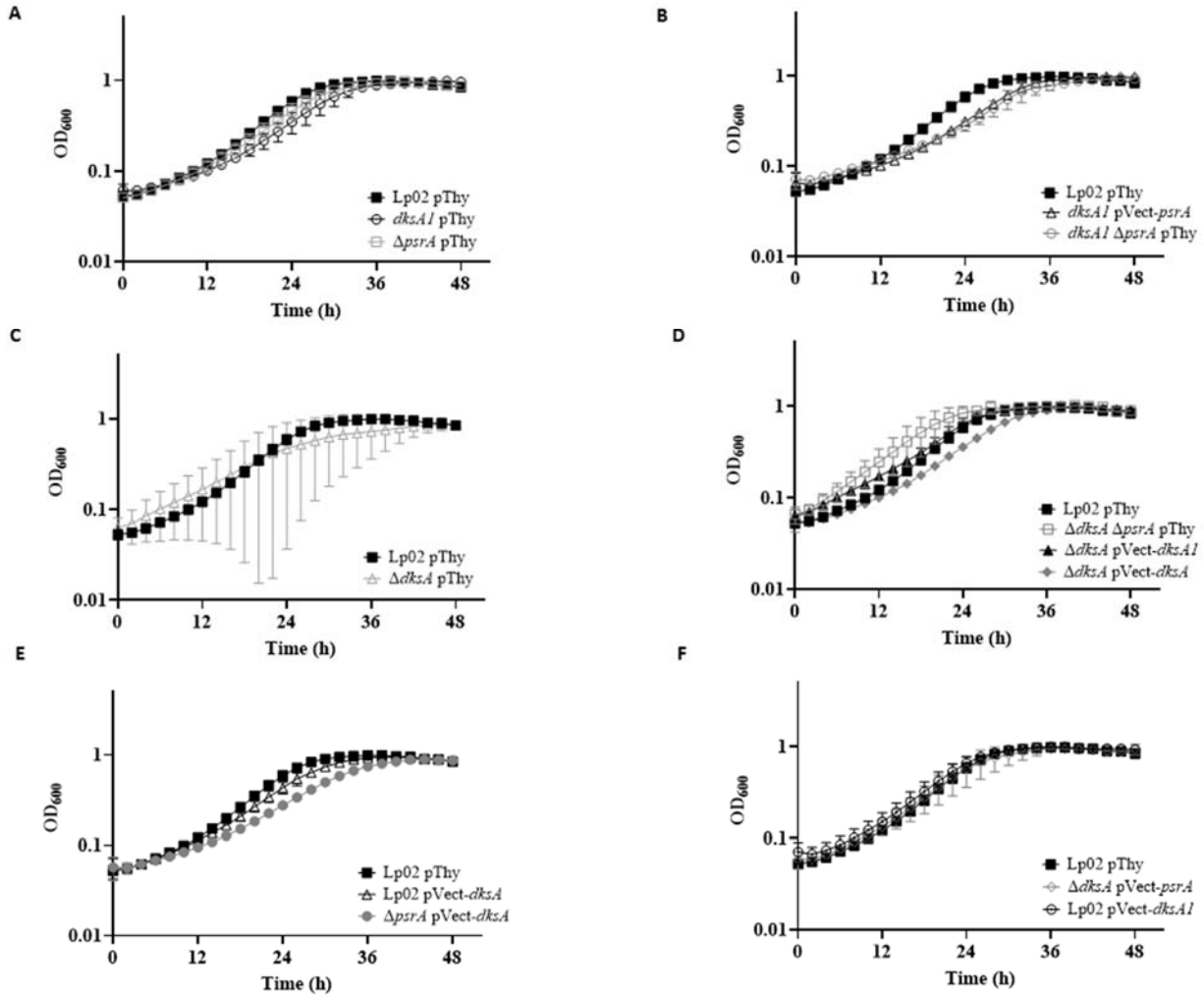

Figure 5: *L. pneumophila in vitro* growth at 25°C is impacted by DksA, PsrA and DksA1. *In vitro* growth kinetics of parental Lp02 and isogenic strains featuring single or combinatorial genetic mutations (Δ*psrA*, Δ*dksA*, *dksA1*) with and without *in trans* expression of *psrA, dksA* or *dksA1* genes. Plate-grown bacteria were re-suspended in BYE broth and normalized to initial OD_{600} = 0.15, and growth at 25°C was monitored for OD_{600} every 2 h for 48 h. Graphs in panels A-F were experiments conducted concurrently, but presented separately for clarity. Error bars are SD across mean of three independent biological replicates with three technical replicates each.

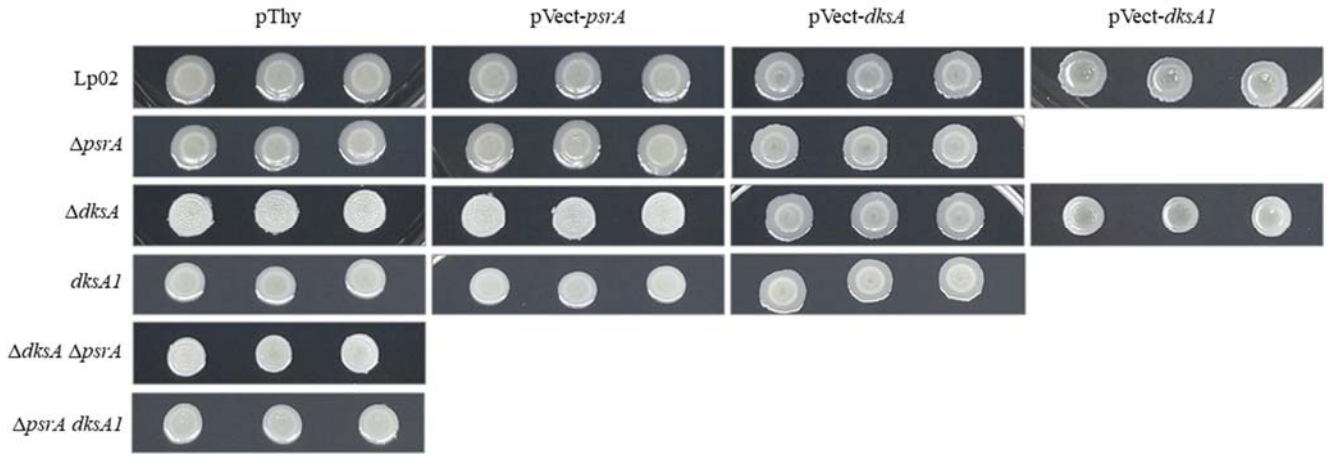

Figure 6: *L. pneumophila* DksA and DksA1, but not PsrA affects colony morphology. Parental Lp02 and isogenic strains featuring single or combinatorial genetic mutations (Δ*psrA*, Δ*dksA*, *dksA1*) with and without *in trans* expression of *psrA, dksA* or *dksA1* genes. Strains were grown on BCYE plates for 3 days and used to generate a bacterial suspension in BYE at OD_{600} = 0.15. 10 µL of the suspension was spotted onto BCYE plates in triplicate then the plates were incubated at 37°C at 5% CO_2 for 4 days prior to being photographed. Images are representative of one of three biological replicates.

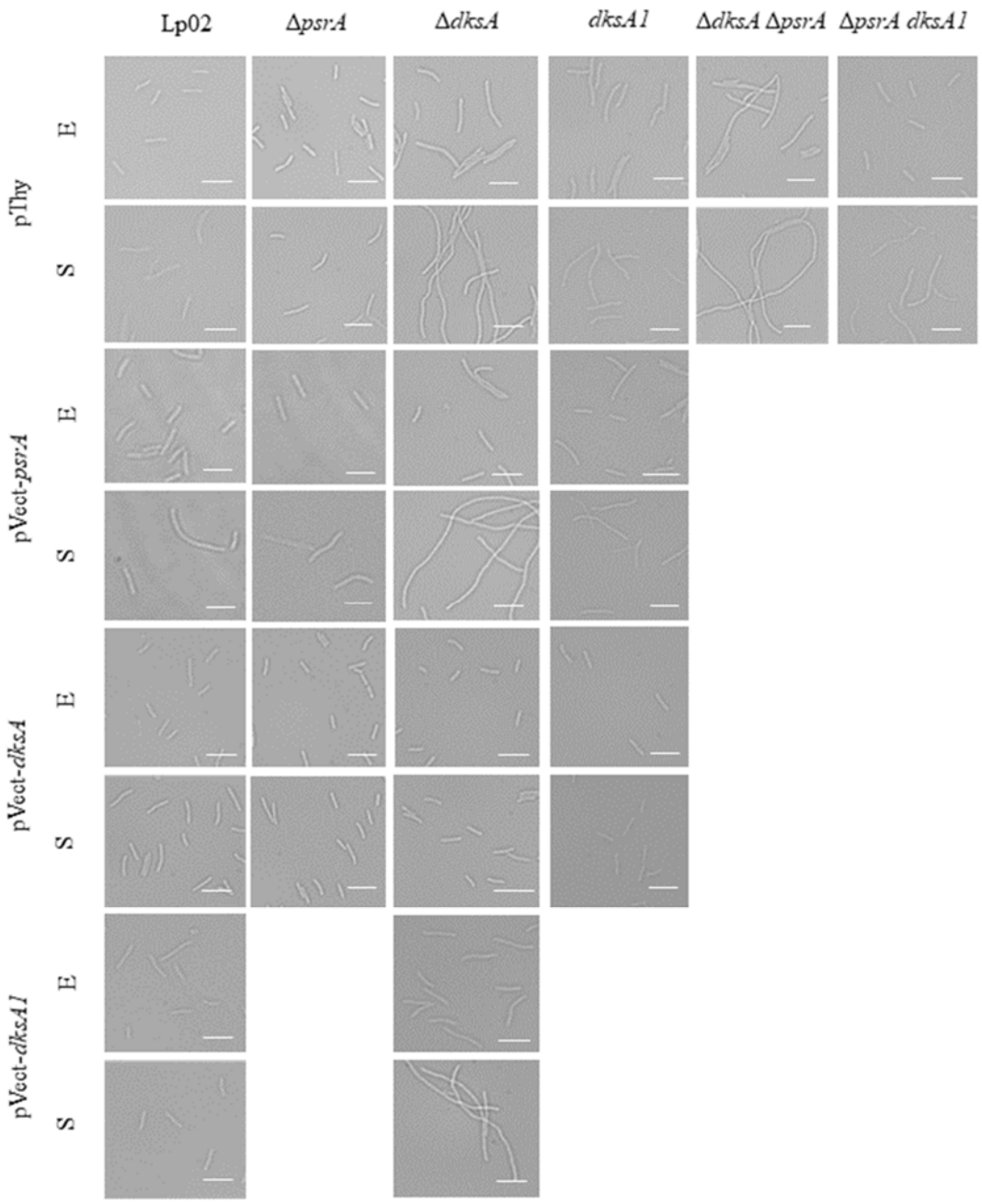

Figure 7*: L. pneumophila* Δ*dksA*, but not *dksA1* or *psrA* cause filamentation. Parental Lp02 and isogenic strains featuring single or combinatorial genetic mutations (Δ*psrA*, Δ*dksA*, *dksA1*) with or without *in trans* expression of *psrA, dksA* or *dksA1* genes were grown on BCYE plates and used to inoculate a dilute suspension of OD_{600} = 0.02 in BYE broth then incubated overnight at 37°C with aeration, to exponential (E) (~18h , OD_{600} = ~0.5) or stationary (S; 24 h after EP) growth phases, then live-mounted on a 2% agarose pad prepared in ddH_2O and imaged on an Axio Observer Z1 inverted microscope (Zeiss) equipped with a glycerol-immersion 150X objective. Representative microscopic images of bacteria from one of three biological replicates. Scale bar is 5 µm.

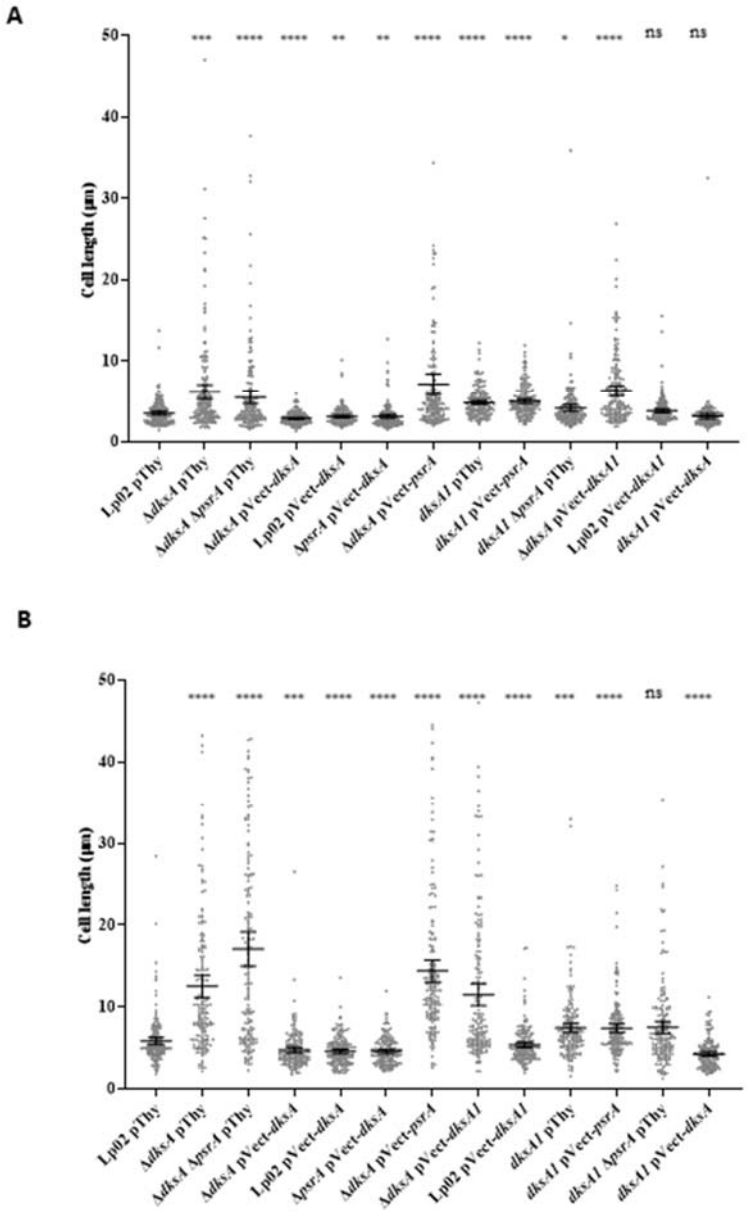

Figure 8*: L. pneumophila* Δ*dksA*, *dksA1*, and *psrA* contribute to cell length regulation. Parental Lp02 and isogenic strains featuring single or combinatorial genetic mutations (Δ*psrA*, Δ*dksA*, *dksA1*) with or without *in trans* expression of *psrA, dksA* or *dksA1* genes were grown from 3-day old plates subcultured to BYE broth at OD_{600} = 0.02 then incubated at 37°C with aeration to (A) exponential (overnight, OD_{600} ~ 0.5) or (B) stationary phases (24 h after exponential phase) then imaged with an Axio Observer Z1 inverted microscope (Zeiss) equipped with a glycerol-immersion 150X objective and individual bacterial cell lengths quantified using the length tool in ImageJ. Where filamentation was evident, only individual cells for which the full length was visible were measured. Data represents >150 individual readings spread equally across three biological replicates. Bar on graph and error bars represents mean and 95% confidence interval, respectively. Statistical significance determined by Student's T-test (*, $p < 0.05$; ** $p < 0.01$; *** $p < 0.001$; **** $p < 0,0001$; ns, not significant, $p > 0.05$).

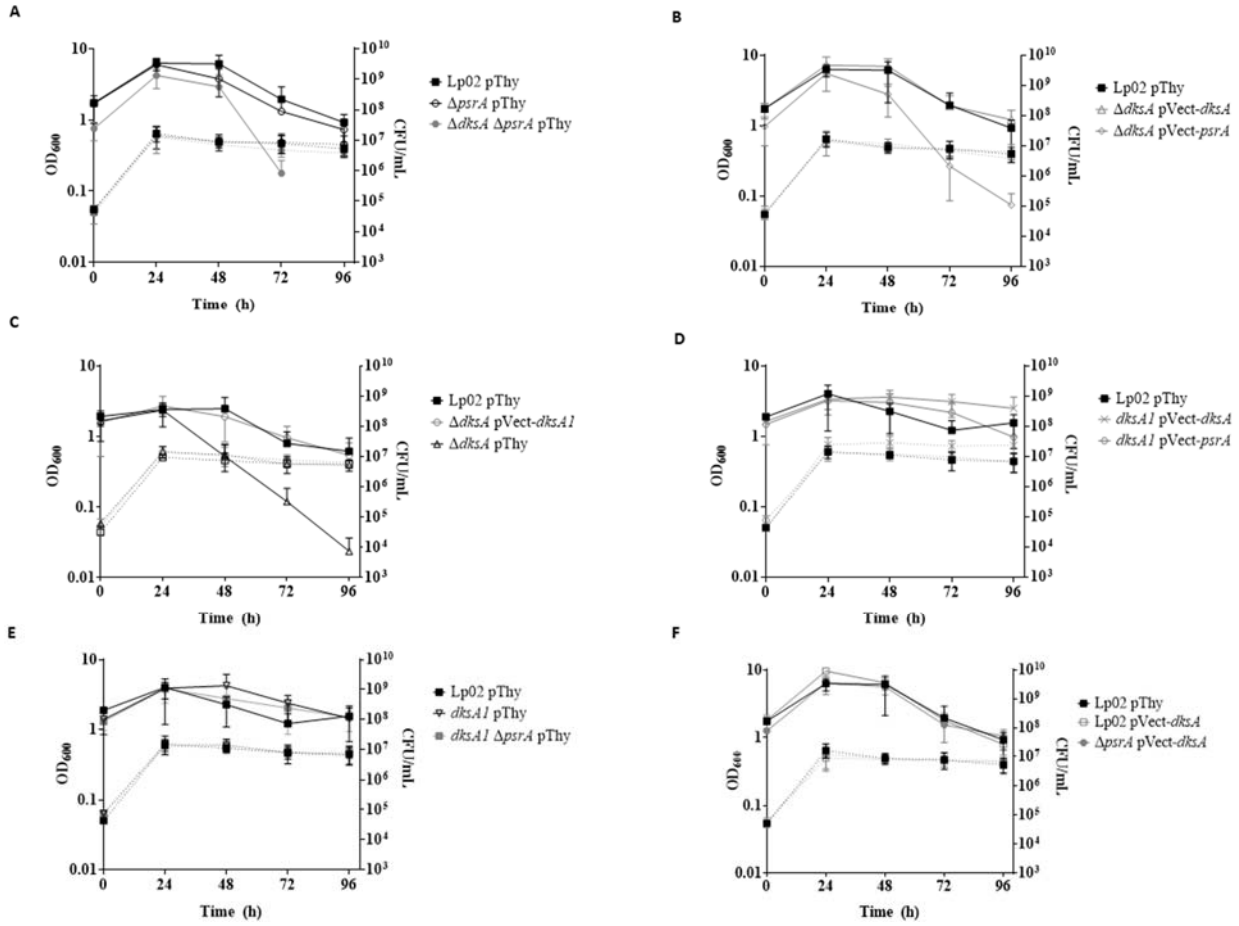

Figure 9: Bacterial culturability in depleted nutrient media is dependent on DksA or DksA1, but not PsrA. Panels (A-F) show *in vitro* growth kinetics of Lp02 and isogenic strains featuring single or combinatorial genetic mutations (Δ*psrA*, Δ*dksA*, *dksA1*) with or without *in trans* expression of *psrA, dksA* or *dksA1* genes in BYE broth at 37°C for 96 hours with OD_{600} values (dotted lines; left Y axis) and titre enumerated by serial dilution and incubation on BCYE plates (solid lines; right Y axis) at 24 h intervals. Data are presented as mean and SD of three biological replicates. Points were omitted if results could not be calculated (no colonies recovered, below detection limit of ~100 CFU/mL). Graphs in panels A-F were experiments conducted concurrently, but presented separately for clarity.

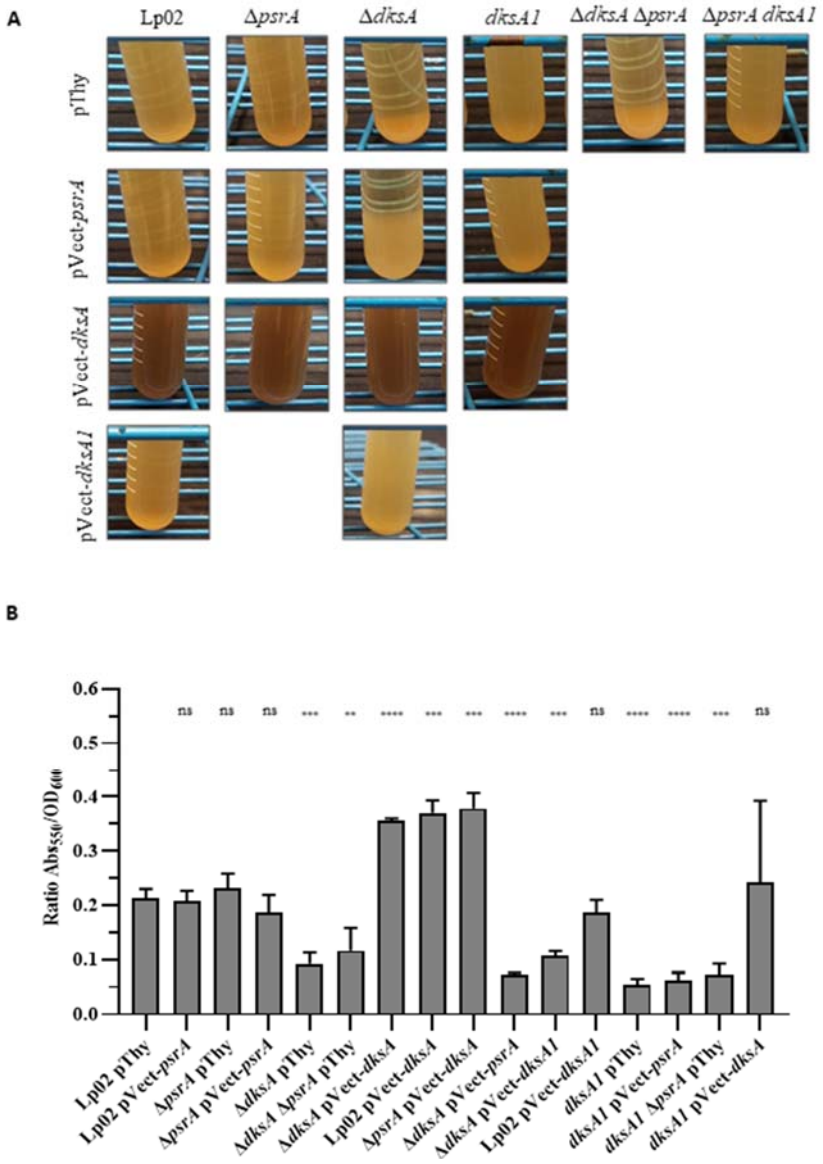

Figure 10: Pigmentation is regulated by DksA, but not PsrA. Parental Lp02 and isogenic strains featuring single or combinatorial genetic mutations (Δ*psrA*, Δ*dksA*, *dksA1*) with or without *in trans* expression of *psrA, dksA* or *dksA1* genes, were grown on BCYE plates for 3 days and used to generate a 5 mL bacterial suspension (BYE at $OD_{600} = 0.15$) then incubated at 37°C for 30 h (a) Qualitative observation of pigmentation. After 48 h incubation tubes were set aside for 24 h at room temperature to allow cells to sediment out, then photographed. Representative image of three replicates. (b) Quantification of pigment at 30 h. After 30 h of incubation 1 mL of culture was centrifuged at 20,000 x *g*. The supernatant was measured for pigment levels via absorbance at 550 nm, then the pellet was resuspended in same volume of 1X PBS pH 7.0 to measure cell density via OD_{600}. Readings were taken with a plate reader in a 96 well plate relative to appropriate BYE or PBS blanks. Readings reflect Abs_{550}/OD_{600}. Error bars represent SD across three biological replicates. Statistical significance calculated via Student's T-Test and relative to parental Lp02 pThy, indicated above bars (*, $p < 0.05$, ** $p < 0.01$; *** $p < 0.001$; **** $p < 0,0001$; ns, not significant, $p > 0.05$).

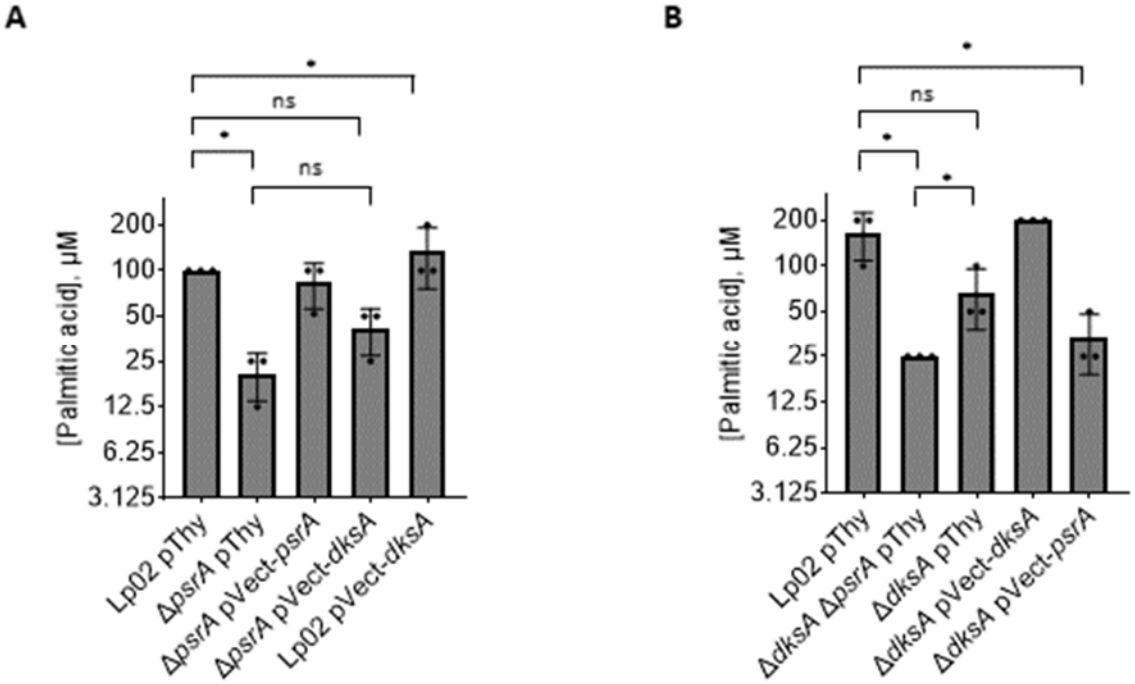

Figure 11: PsrA and DksA influences LCFA-mediated growth inhibition. Parental Lp02 and isogenic strains featuring single or combinatorial genetic mutations (Δ*psrA* and/or Δ*dksA*), with or without *in trans* expression of *psrA* or *dksA* genes, grown with and without palmitic acid supplementation (as 40 mM stock dissolved in ethanol) in BYE media normalized to 0.5% ethanol, in a 96-well microplate for 24 h with shaking at 37°C. Inhibition was defined as growth, as assessed by OD_{600} values, of <50% of that of same strain in a BYE + 0.5% ethanol-only control at the end of 24 h. Bars indicate mean of maximum concentration of PA where indicated strain grew >50% of maximum, over three biological replicates with standard deviation indicated. Dots in bars indicate individual replicate values. Panels A and B were conducted separately. Statistical analyses were done using Student's unpaired T test: ns = no significance, * = $p<0.05$.

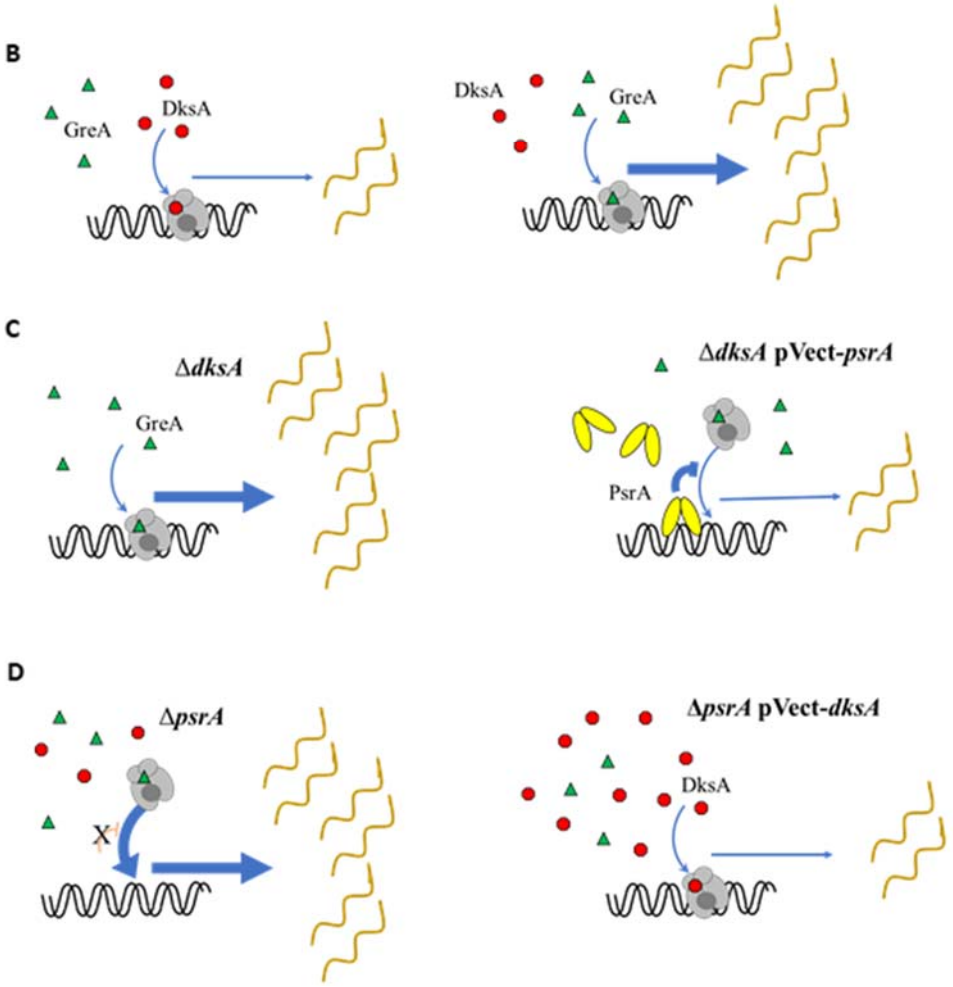

Figure 12: Model of independent mechanisms of DksA and PsrA. A hypothetical promoter is repressed by both PsrA and DksA (A) RNA polymerase (RNAP) holoenzyme is targeted to -10 and -35 boxes by a sigma factor. PsrA (oval dimers) binds a defined site in the promoter and inhibits RNAP recruitment. (B) RNAP binds to GreA (triangles) or DksA (filled octagons) interchangeably, with enhanced transcription initiation rates occurring while bound to GreA versus DksA. (C) In a Δ*dksA* strain, only GreA is available for RNAP thus elevating transcription levels, but *in trans psrA* overexpression generates higher levels of PsrA, strengthening inhibition of RNAP recruitment to compensate. Conversely (D) the Δ*psrA* strain allows uninhibited RNAP-promoter binding, increasing transcription, but this is offset by overexpressing *dksA in trans*, increasing the proportion of RNAP bound to transcription-inhibiting DksA thereby generating the compensatory effect.